AGENCY FOR INTERNATIONAL DEVELOPMENT
WASHINGTON, D. C. 20523

BIBLIOGRAPHIC INPUT SHEET

FOR AID USE ONLY

1. SUBJECT CLASSIFICATION

A. PRIMARY: Agriculture

B. SECONDARY: Irrigation

2. TITLE AND SUBTITLE

Trickle-drip irrigation: principles and application to water management in tropical soils

3. AUTHOR(S)

Bresler, Eshel

4. DOCUMENT DATE	5. NUMBER OF PAGES	6. ARC NUMBER
1975	81 p.	ARC

7. REFERENCE ORGANIZATION NAME AND ADDRESS

Department of Agronomy, Cornell University, Ithaca, New York 14853

8. SUPPLEMENTARY NOTES *(Sponsoring Organization, Publishers, Availability)*

(In Agronomy mimeo 75-14)

9. ABSTRACT

This series of lectures presents the known general principles of trick irrigation systems. It then applies the principles to the design of a trickle irrigation system for three representative soils of the tropics, from Puerto Rico and Brazil, using soil hydraulic data and crop response information obtained by Wolf and Drosdoff (1974) and Wolf (1975). The use of trickling or dripping as a method of irrigating large fields has become quite common practice all over the world the method is now one of the fastest growing new technologies in agriculture. U.S. acreage under drip irrigation has increased from 100 acres in 1970 to more than 70,000 acres in 1974. The five-year projection is for over 218,000 acres in the U.S. and for at least 100,000 acres in other countries. Trickle irrigation is being adapted to almost all types of crops and all types of land, including land which could not be used previously for successful agriculture. The topics discussed in this publication include the following: important features of trickle irrigation; some problems concerning practical use; modeling of water and salt flow; soil water regime during infiltration; application of infiltration models to the design of a trickle irrigation system; and application to water management in tropical soils.

10. CONTROL NUMBER	11. PRICE OF DOCUMENT
PN-AAB-870	
12. DESCRIPTORS	**13. PROJECT NUMBER**
Drip irrigation?	
Trickle irrigation	**14. CONTRACT NUMBER** CSD-2834 211(d)
Tropics	**15. TYPE OF DOCUMENT**

AID 590-1 (4-74)

CSD-2834 211(d)
PN-AAB-870

TRICKLE-DRIP IRRIGATION: PRINCIPLES AND APPLICATION TO WATER MANAGEMENT IN TROPICAL SOILS

A Series of Lectures at the

Department of Agronomy, Cornell University

by

Eshel Bresler, Visiting Associate Professor

Agronomy Mimeo 75-14

Department of Agronomy

Cornell University

Ithaca, New York 14853

July 1975

Supported in part by grant csd 2834 to Cornell University by the Agency for International Development under the Institutional Grants Program established by Section 211(d) of the Foreign Assistant Act of 1961 as amended in 1966.

TABLE OF CONTENTS

	Page
Introduction	1
Important Features of Trickle Irrigation	4
Improving soil-water regime for greater crop yield	4
Minimizing the salinity hazard to plants	8
Partial wetting of the soil volume	8
Maintaining dry foliage	10
Flexibility in fertilization	10
Possible water saving	11
Technical-economical features	11
Some Problems Concerning Practical Use	13
Clogging	13
Salinity problems	13
System design problems	14
Technical improvements	15
Modeling of Water and Salt Flow	16
The physical system	16
Governing equations	18
Water flow boundary conditions	20
Axisymetric-cylindrical flow models	23
Plane flow model	25
Solutions	26
Comparison with experimental data	27
Soil Water Regime During Trickle Infiltration	33
Solute Distribution During Infiltration	40
Application of Infiltration Models to the Design of Trickle Irrigation System	47
Steady infiltration from a circular pond	48
Estimation of the radius of the ponded area ρ_u	51
Estimation of spacing between emitters	52
Numerical evaluation	55
Application to Water Management in Tropical Soils	59
Estimations of soil-water parameters	61
Spacing between emitters as a function of discharge and midway pressure	63
Irrigation scheduling	69
Design the lateral system	73
Literature Cited	76
Appendix - Notations Used	79

TRICKLE-DRIP IRRIGATION: PRINCIPLES AND APPLICATION TO WATER MANAGEMENT IN TROPICAL SOILS

by

Eshel Bresler, Visiting Associate Professor[1]
Department of Agronomy, Cornell University

INTRODUCTION

The use of trickling or dripping as a method of irrigating large fields has become quite common practice in agricultural production all over the world. The method is now one of the fastest growing new technologies in agriculture. The amounts of acreage where it is being used throughout the U.S.A. and the whole world are steadily increasing. The area under drip irrigation in the U.S.A. was 100 acres in 1970 and over 70,000 acres in 1974. Moreover, the anticipated five-year projection is for over 218,000 acres in U.S.A. and for at least 100,000 acres in other countries (see Table 1). Trickle irrigation is being adapted to almost all types of crop production (strawberries to large scale sugarcane), all types of land (level land planting of row and tree crops to steep hill-side planting of fruit crops) even those which previously could not be used for successful agriculture.

The complete trickle irrigation system consists of emitters which distribute the water for irrigation and are attached to laterals to which water is delivered through the submains or main lines. The trickle emitter is esentially a water energy reducer. It acts generally as a resistor which dissipates the energy of water flowing through it and thus reduces

---

[1]Associate Professor, Department of Soil Physics, Institute of Soils and Water, Agricultural Research Organization, Volcani Center, Bet-Dagan, Israel, and Hebrew University of Jerusalem, Faculty of Agriculture, Rehovot, Israel.

Table 1. Drip irrigation survey (after Gustafson *et al.*, 1974).

State or Country	Present Acreage	5-Year Estimate
U.S.A.		
Alabama	7	----
Arizona	5,000	50,000
California	40,000+	100,000+
Colorado	5	----
Connecticut	0	----
Delaware	5	Very promising
Florida	6,000	10,000+
Georgia	82	----
Hawaii	12,500	25,000+
Indiana	40	500
Kentucky	5	----
Louisiana	20	200
Massachusetts	0	----
Michigan	3,000	6,000
Minnesota	0	100
Mississippi	0	0
Missouri	60	300
Nebraska	2	----
New Mexico	400	700
New York	150	2,000
North Carolina	30	----
North Dakota	1	----
Ohio	5	----
Oregon	325	10,000
Pennsylvania	55	----
Rhode Island	0	----
South Carolina	12	----
South Dakota	2	----
Texas	3,000	6,500
Utah	100	500+
Washington	1,000	5,000+
TOTAL ACRES	71,816+	216,800+
FOREIGN		
Australia	25,000	60,000
British Columbia, Canada	500	----
Central America	700	----
Cyprus	400	3,000
Israel	15,000	----
Mexico	16,000	----
New Zealand	2,000	----
South Africa	8,600	30,000
Other Countries	3,000	----
TOTAL ACRES	71,200	93,000

the flow rate. The water energy is reduced by means of an orifice and is increased by the length of the water flow path by means of screw-like plastic tube or by means of a porous material. Generally, water enters the dripper, travels the length of the path which reduces its pressure, and discharges as a trickle at a controlled rate. The flow rate is controlled by the pressure distribution which in turn is determined by size and type of dripper and the water carrier.

The surface approach, as opposed to underground application of trickling (subsurface irrigation) was initiated in Israel and has been successfully and widely used for the past few years. In the surface approach the irrigation emitter is placed directly on the soil surface so that the area across which water infiltration takes place is small compared with the total soil surface of the irrigated field. As a result one has a case of three-dimensional irrigation. This differs from the usual one-dimensional flooded or sprinkler irrigation where the area across which irrigation water enters the soil is considered to be identical to the total area of the irrigated field. Optimal irrigation criteria are achieved by adjusting the trickling system to the soil hydraulic properties and to the water and nutritional requirements of the specific crop grown. This is done by selecting the best known combination of all constituents which comprise the trickle irrigation system.

In this series of lectures the known general principles of trickle irrigation system are presented. These principles are then applied to the design of a trickle irrigation system for three representative soils of the tropics from Puerto Rico and Brazil using soil hydraulic data and crop response information obtained by Wolf and Drosdoff (1974) and Wolf (1975).

POSSIBLE ADVANTAGES OF TRICKLE IRRIGATION

The traditional methods of water application to the soil have advanced from simple flood irrigation, through furrow irrigation, to a scientifically-controlled sprinkler irrigation system. Each of the conventional irrigation methods has certain advantages and limitations when one considers their technical, economic, and crop production values. The trickle irrigation method has been developed for specific conditions of an intensive irrigated agriculture. Some of the technical and agronomic advantages that may be achieved by selecting the trickling method are given below.

Improving soil-water regime for greater crop yield

The traditional irrigation cycle under furrow, flood, or portable sprinkler system consists of a relatively short period of infiltration followed by a long period of simultaneous redistribution, evaporation, and extraction of water by the growing plants. In this mode of irrigation there is a fixed cost associated with each water application and therefore one's goal is to minimize the number of irrigations by increasing the time interval between two successive irrigations without causing an economic yield reduction. To minimize irrigation frequency the usual goal was to maximize the quantity of available water stored in the soil for subsequent water use by the crop before the next irrigation. The economic constraint of the traditional irrigation methods which cause extremely large time fluctuation in the soil water potential (Bresler and Yaron, 1972) has been partly removed by the development of trickle

irrigation systems capable of delivering water to the soil in small quantities as often as desired with no additional cost.

As the frequency of irrigation increases, the time-average soil water potential increases and is restricted to a narrow range hence eliminating low average soil water content and high water fluctuations as factors affecting plant growth and crop yields. This increase in soil water potential (or decrease in the total soil water suction) at very frequent, or continuous water application is a consequence of both high average matric potential and low soil solution concentration resulting from the fact that the salinity of the soil solution approaches that of the irrigation water. Ayers et al. (1943), Wadleigh and Ayers (1945) and Wadleigh et al. (1951) suggested that matric and osmotic potentials are additive in their effect on plant growth. There is some evidence to support the view that crop yield of many crops is increased by maintaining the soil-water regime at high time-average values of soil water potential in the effective root zone (Rawitz, 1970; Hillel, 1972). This suggests that crop yield may be highly increased by very high irrigation frequency.

The maintenance of continuously high water potential, thus minimizing fluctuations in the soil water contents during the irrigation cycle, may be an important feature of trickle irrigation if one considers the yield response curve to water to be convex and the effect of flucutation in the water status on the crop yield to behave similar to Zaslavsky's (1972) theory as follows.

It is a well-established assumption (e.g. Taylor, 1952) that crop yield depends on both the average of some index of the soil water regime $\bar{\Phi}$ and the time deviations from $\bar{\Phi}$. Generally, this can be expressed as

$$Y(\Phi) = Y[\bar{\Phi}, \phi(t)] \qquad [1]$$

where Y is crop yield, Φ is the soil water index (e.g. sum of matric and osmotic potentials), $\bar{\Phi}$ being its time average (assuming uniform Φ with respect to space), t is time and ϕ is the time (daily) deviation of $\Phi(t)$ from $\bar{\Phi}$, i.e.

$$\phi(t) = \Phi(t) - \bar{\Phi} \qquad [2]$$

Note that when there are no fluctuations in Φ (i.e. $\phi = 0$) then $\Phi(t) = \bar{\Phi}$ and the yield response function to water becomes

$$Y = Y(\Phi = \bar{\Phi}, 0) = Y_o(\bar{\Phi}) \qquad [3]$$

where Φ is perfectly uniform at the $\bar{\Phi}$ level.

Expanding $Y(\Phi)$ function about $\Phi = \bar{\Phi}$ by Taylor's series and neglecting third order and higher terms, we obtain

$$Y(\bar{\Phi} + \phi) = Y_0(\bar{\Phi}) + \phi(t) \frac{\partial Y}{\partial \Phi} (\bar{\Phi}) + \frac{[\phi(t)]^2}{2} \frac{\partial^2 Y(\bar{\Phi})}{\partial \Phi^2} \qquad [4]$$

Averaging the yield over the time

$$Y = \frac{1}{T} \int_{t=0}^{T} Y dt = Y_o(\bar{\Phi}) + \frac{(\partial Y/\partial \Phi)}{T} \int_0^T \phi(t) dt + \frac{(\partial^2 Y/\partial \Phi^2)}{T} \int_0^T [\phi(t)]^2 dt \qquad [5]$$

The first term on the right-hand side (RHS) of [5] is identical to [3] i.e. yield response function without fluctuation in Φ; the second term on the RHS of [5] vanishes upon averaging because average deviations are zero. Since the integral $\frac{1}{T} \int_0^t [\phi(t)]^2 dt$ is the mathematical definition of the variance σ^2 therefore

$$\bar{Y} = Y_o(\bar{\Phi}) + \frac{\sigma^2}{2}\frac{\partial^2 Y}{\partial \Phi^2} \qquad [6]$$

Here again Y is the yield, $\bar{Y}$ being average yield, Φ is the water regime index (e.g. sum of matric and osmotic potentials), $\bar{\Phi}$ being its average over the time and σ^2 is the variance of Φ. Note that the first term on the RHS of [6] is the yield that would have been obtained with perfectly uniform levels of Φ all at the average $\bar{\Phi}$ (yield without fluctuations), and the second term is the first correction to the yield due to fluctuations (fluctuation contributions). Note also that if the $Y(\Phi)$ function is convex then the second derivative in [6] is negative and time fluctuations in the soil water potential will cause crop yield reduction. Generally, $\partial^2 Y/\partial \Phi^2 < 0$ and thus, fluctuations of soil water content with time have a negative effect on the crop yield. If this is indeed the general case, then the best irrigation policy is to apply the water as frequently as possible as long as there are no aeration problems. Referring to eq. [6] it is clear that a direct relationship exists between crop yield and irrigation frequency if the yield response to soil water potential would have been a convex monotonic increasing function. With trickle irrigation method, capable of delivering water to the soil as often as desirable with no additional costs, this potentiality in increasing crop yield can be obtained. It is possible, therefore, to draw a conclusion that if the views expressed by eq. [6] (Zaslavsky, 1972) would have consistently been supported by experimental evidence, then optimizing the soil water regime for greater crop yield is the most important feature of trickle irrigation method.

Minimizing the salinity hazard to plants

Recent work by Bernstein and Francois (1973) shows that brackish irrigation water with 2450 mg/liter total salts can successfully be used with drip irrigation to obtain almost the same yield as nonsaline good quality water. Using the same water for furrow and sprinkler irrigations caused yield reduction of 54 and 94 percent, respectively. Increasing the irrigation frequency caused only 18 and 59 percent reduction in yield for furrow and sprinkler irrigation, respectively. Minimizing the salinity hazard to plants irrigated by trickling can be related to: (a) the displacement of salts beyond the main efficient root zone; (b) lowering the salt concentration by maintaining a relatively high soil water content due to the high frequency irrigation; and (c) avoiding leaf burning and damage due to salt accumulation on the surface of leaves which are in contact with irrigation water. However, Bernstein and Francois (1973) attributed the low yields and injury by sprinkling as compared with trickling to the osmotic shock caused by flushing the salt, which had accumulated at the soil surface between two successive irrigation, into the root zone rather than to the foliage adsorption of salt. Similar shock can be observed in drip irrigation when the salt which accumulates in the periphery of the wetted soil volume, midway between emitters, is washed by rain into the main root zone.

Partial wetting of the soil volume

An additional feature of trickle irrigation is the possibility of restricting water supply to those parts of the soil where the activity of the root system, with respect to water and nutrient, is the most efficient. Bernstein and Francois (1973) found that many of the roots under trickle

irrigation occur in the surface 2.5 cm soil, except when salt accumulation inhibits root development. Black and West (1974) tested the effect on water use of young apple trees when varying proportions of the root systems were supplied with an "optimum" water regime. They found that when the fraction of the wetted root system was decreased from 1.0 to 0.25, the relative transpiration reduced from 1.0 to only 0.75. Their results also suggested that wetting substantially less than the total root system daily would produce at least as good regime for plant water supply as wetting the entire root system with a 14-day interval between irrigations. Glasshouse and growth cabinet experiments (Frith and Nichols, 1974) showed that local application of water to less than the total root volume did not affect the ability of the tree to take up sufficient water, and that roots in the wetted root zone increased their ability of water uptake.

It was also found that a portion of the root system could, if required, assimilate as much nitrate-nitrogen as the whole root system. This experimental finding is of practical importance since satisfactory nutrition can be obtained by dissolving fertilizers in the trickle irrigation water and the roots in the wetted root zone should increase their efficiency of nutrient uptake in a manner similar to their increasing efficiency in the water uptake. Thus, under trickle irrigation it is possible for trees to have their root volume wetted considerably less than the total root system. The ability of peach trees to quickly and profoundly adapt its root system to the partial wetting pattern of trickle irrigation is also of interest. A whole new root system for large trees (5.8 m wide and 5 m high) was developed in a few months and the tree continues to produce heavy cropping yields (Willoughby and Cockroft, 1974).

Selective wetting of the soil surface has additional beneficial results such as reducing water evaporation by preventing evaporation of water from outside of the wetted surface zone. The partial wetting also restricts the growth of weeds to the wetted region and thus causes a reduction in the cost of weed control by decreasing the need for weed control beyond the wetted region. The wet spots then may be controlled very efficiently by applying herbicides through the dripping system. More convenient pest control is also obtained by leaving dry strips in which the pest control machinery can easily be moved.

Maintaining dry foliage

Dry foliage causes a retardation in the development of leaf diseases that require humidity. It does not necessitate the removal of plant-protecting chemicals from the leaves by washing. This is of course in addition to the prevention of leaf burns due to the lack of direct contact of the leaves with saline irrigation water.

Flexibility in fertilization

Trickle irrigation offers flexibility in fertilization that is unique to this system. Since fertilization can easily go along with irrigation, frequent or continuous application of nutrients at low concentrations is applicable and seems to be a very good practice. Optimizing the nutritional balance of the root zone is possible by supplying the nutrients directly to the most efficient part of the root zone. Other features include good fertilizer distribution with minimum leaching beyond the root zone and more options in the timing of fertilizer application than in any other distribution system. However, the fertilizer mixtures must be completely soluble in water and must not leave any residues in the fertilizer dispenser

and also must not cause clogging of emitters.

Possible water saving

There are several ways by which water may be saved in using trickle irrigation as compared with the other traditional irrigation methods. Under trickle irrigation loss of water due to runoff in low permeable or crusted soils is reduced. In addition, destruction of the surface-soil structure and the development of surface crust is avoided and water infiltration into the soil is largely improved.

Much water saving may be achieved by restricting the water supply to the extent of the most efficient root zone. By not wetting the entire inter-row or inter-tree space, especially in young crops or trees, direct evaporation from the soil surface and water uptake by weeds are drastically reduced. On steep hills and/or under severe wind blowing conditions furrow and sprinkle irrigation methods are very inefficient with respect to water saving. Under these conditions, the use of trickle irrigation prevents water loss beyond the border of the irrigated field by wind convection or runoff in contour cultivation on steep hills.

Technical-economical features

Labor and water resources constitute a major concern for the development of this new approach of irrigation. In many countries and instances where labor and water became limiting and expensive, the method of trickle irrigation has been developed. Automation is one of the very reliable tools which can easily be used in trickle irrigation for accurate soil

water control, supplying of water as needed and largely reducing the use of manpower. A simple automation system includes an automatic timer that can be set for daily operation at certain hours of the day. More sophisticated units can be controlled by electrified tensiometers in the root zone by having an electrical impulse trigger of the system when the matric potential is reduced to a certain dryness.

These days when energy supply becomes limited and expensive, optimal irrigation method should also rely on a relatively low operational pressure which is one of the main technical features of the trickling method. Additional important technical-economical feature of trickle irrigation is the use of a small pipe diameter and the possibility of operating the system 24 hours a day, including windy hours. Frequent irrigation during the windy hours protect sensitive and high investment crops from desiccation without wasting water by wind convection.

Another economical-technical feature of the trickle irrigation system is the reduced cost of weed control. This is so because weeds grow only in the wetted spots and weed control may be obtained through the trickling system. The use of herbicides through the irrigation system offers an answer to weed problems under trickle irrigation especially if one uses herbicides capable of killing weeds as they germinate (Lange et al., 1974). Another aspect of trickle irrigation in relation to the economy of pest control is the possibility of using the soil fungicides in the irrigation system in order to control root rot fungus (Zentmeyer et al., 1974).

SOME PROBLEMS CONCERNING PRACTICAL USE

Trickle irrigation has been developed with the aforementioned features in mind. The technical and agronomical objectives in selecting this method have been already discussed. However, some problems concerning the practical use of the method still exists, and part of them will be discussed.

Clogging

Operational difficulties of trickling method may sometimes arise from the clogging of the drippers, which causes the most severe maintenance problem. Clogging affects nonuniform water distribution and requires frequent replacement of emitters which is a quite expensive procedure. Clogging is caused by several factors such as: a) root penetration; b) blockage of orifice by sand, rust, leaves, small soil animals, microorganisms, etc.; c) precipitation of soluble salts such as carbonates, iron, aluminum and phosphate compounds. Smaller particles can pass through the filtering system and act as crystallization nuclei in the trickling system. Overcoming the clogging-caused difficulties involves the use of a very efficient filtering system and periodically cleaning or replacing the drippers. This, of course, involves some extra expenses and manpower especially when a large number of emitters and laterals per unit area is needed.

Salinity Problems

In arid regions where saline water must be used there is a tendency for salt to accumulate close to the margins of the wetted zone (see Figure 10). The salt which tends to accumulate in the soil midway between emitters may

be washed by rain into the effective root zone and may cause osmotic shock to plants (Bernstein and Francois, 1974). The accumulation of salt at the periphery between emitters could be a serious problem also for seasonal crops, because part of the newly sown plants may fall in regions of high salt concentration from the previous crop. This salt must therefore be leached before the next crop is going to be planted. In areas where there is not sufficient rainfall for the leaching process then leaching must be accomplished by sprinkler or flood irrigation, which increases the cost considerably. Another expensive solution is to place the emitters in much closer spacing in order to approach one dimensional vertical flow. With high frequency irrigation it is also possible to apply water in excess of evaporatranspiration in order to leach the accumulated salt out of the root zone and thus to control soil salinity. Controlling the quantity of water passing through the root zone to avoid salinity buildup is one of the problems of trickle irrigation.

System design problems

In sprinkle irrigation method when one-dimensional water flow takes place there are no severe design problems. The spacing between sprinklers and operational pressure are designed in such a way as to meet certain uniformity criteria. Irrigation scheduling is designed by taking into account one-dimensional evapotranspiration and effective rooting depth. In trickle irrigation when three-dimensional flow occurs the main design problem is to select the proper combination of emitter spacing and discharge for a given soil and crop.

In cases where there are no salinity problems, the wetted volume of soil should be kept within the borders of the efficient root zone. In

order to prevent losses of water beyond the efficient root zone one must determine the proper combination of emitter spacing and discharge, irrigation frequency, and amount of water applied for a given set of soil water characteristics, crop root distribution, water distribution prior to each irrigation, and the pattern of water uptake by roots. Determinations of the proper emitter spacing and discharge under given external conditions require knowledge of soil hydraulic properties together with crop response to size and form of the wetted soil volume and to the water distribution and fluctuation within this volume.

Technical improvements

Technical improvements include the following aspects: 1) mechanical improvements of emitters, various fittings, and filters, 2) finding chemical and other treatments to eliminate mechanical and chemical clogging of emitters and failure of the operation system, and 3) development of a good fertilization system. In addition, development of portable trickle irrigation system and cheaper components would make the method more suitable to irrigate close-planted crops, which are sensitive to the water distribution in the soil.

MODELING OF WATER AND SALT FLOW

Mathematical models are used to approximate physical conditions by mathematical equations. When the equations are too complicated to be solved analytically, their solutions are performed with the aid of a computer. Several phases are involved in the development of the model. These are: a) identification of the relevant physical problems and the mathematical model that can simulate the physical problem; the physical parameters that are included in the model must be determined separately and independently; b) mathematical formulation of the governing equations and the boundary conditions of the problem; c) development of a method of solution in order to solve the mathematical problem; d) verification of the model by first, a comparison between exact analytical solutions and the approximate model solution, and second by performing physical experiments and comparing the theoretical results with field or laboratory observations; e) efficient implementation of the procedure on the computer; f) compatability of the final product with existing models, if there are such models.

The physical system

The irrigation system to be considered in this chapter consists of a small screwshaped plastic tube, fitted into an outer case. Water enters through an orifice, travels the length of the spiral path, which reduces its pressure, and discharges out as a trickle at a predetermined rate. The irrigation trickle nozzle is placed directly on the soil surface, so that the area across which infiltration takes place is very small compared with the total soil surface. As a result, one has a case of three-dimensional, transient infiltration of water into the soil. This differs from the usual one-dimen-

sional case of flood or sprinkler infiltration, where the area across which water enters the soil is assumed to be identical to the entire soil surface.

As mentioned earlier, one of the important goals of trickle irrigation is to maximize the time-average soil water potential by increasing irrigation frequency. As the frequency increases, the infiltration period becomes more and more important and the irrigation cycle is changed from an extraction-dominated process to an infiltration-dominated process (Rawlins, 1973). Because in trickle irrigation, when irrigation is sufficiently frequent, the irrigation cycle is dominated by the infiltration stage, the discussion here is limited to the modeling of the problem of salt and water flows during infiltration only.

Consider a field that is irrigated by a set of emitters or trickle sources, spaced at regular intervals, 2X and 2Y, as shown in Figure 1. Due to the symmetry of the pattern, one can subdivide the entire field into identical volume elements, W, of length X, width Y, and depth Z, where the latter always remains below the wetting front. Here, each volume element acts as an independent unit in the sense that there is no flow from one element to another. Therefore, in order to describe the salt and water flows in the entire field, it is sufficient to analyze their status in a single element, W. This, of course, is true only for the interior part of the field that is not too close to the margins.

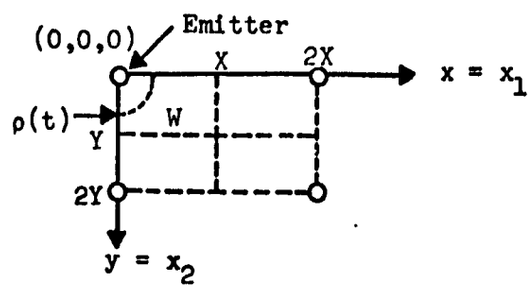

Figure 1. Schematic representation of trickle irrigated field.

Governing equations

The differential equations governing the flow of water and noninteracting solutes in an unsaturated soil system can be written in indicial notation as (cf. e.g. Neuman, 1973; Bear, 1972).

$$\frac{\partial\theta}{\partial t} = \frac{\partial}{\partial x_i}\left[K^r(\theta)K^s_{ij}\frac{\partial p(\theta)}{\partial x_j} + K^r(\theta)K^s_{i3}\right] \qquad [7]$$

$$\frac{\partial(c\theta)}{\partial t} = \frac{\partial}{\partial x_i}\left[D_{ij}\frac{\partial c}{\partial x_j} - q_i c\right] \qquad [8]$$

Here x_i $(i = 1,2,3)$ are spatial coordinates (x_3 the vertical), $0 < K^r \leq 1$ is the relative hydraulic conductivity (Neuman, 1973), K^s_{ij} is hydraulic conductivity tensor at saturation, θ is volumetric soil water content, t is time, p is pore water pressure head, D_{ij} is coefficient of hydrodynamic dispersion (combining the effects of diffusion and mechanical dispersion), q is specific flux of the solution, and c is solute concentration in the soil solution. Equations [7] and [8] are written in an indicial notation such that quantities with a single subscript, or index, represent components of vectors, quantities with two subscripts are component of tensors, and when an index appears twice in any given term this term must be summed over all admissible values of that particular index (such as i and j in [7] and [8]).

In analyzing the problem of transient infiltration from a trickle source, we shall assume that the soil is a stable, isotropic and homogenous porous medium and that Darcy's law applies in both the saturated and unsaturated zones. Under these assumptions, and considering only two space dimensions $x_1 = x$, and $x_3 = z$, eq. [7] that governs the flow of water in the system can be expressed as

$$\frac{\partial\theta}{\partial t} = \frac{\partial}{\partial x}\left[K(\theta)\frac{\partial p}{\partial x}\right] + \frac{\partial}{\partial z}\left[K(\theta)\frac{\partial H}{\partial z}\right] \qquad [9]$$

Here, x is the horizontal coordinate, z is the vertical coordinate (considered to be positive downward), $K(\theta) = K^r(\theta)K^s$ is the hydraulic conductivity of the soil (depending on θ alone), and H is the hydraulic head (sum of pressure head, p, and gravitation head-z). Note that eq. [9] considers the water pressure head p and the hydraulic conductivity K to be single-valued, continuous functions of θ and the hydraulic gradient to be the only force causing water to flow.

The form of the dispersion term D_{ij} in eq. [8] has been the subject of intense discussion. Recent experimental and theoretical studies (Ogata, 1970; Perkins and Johnson, 1963; Bear, 1972) suggest that in isotropic and homogenous porous media the principal axes of dispersion are oriented parallel and perpendicular to the mean direction of flow. This indicates that for such media the transport of the dispersed material can be defined by two characteristic dispersion components that are specified when the mean direction of flow is known. Let D_{ij} for an isotropic media be defined similar to Bear (1972, p. 612) as

$$D_{ij} = \lambda_T|V|\delta_{ij} + (\lambda_L - \lambda_T)\, V_i V_j/|V| + D_p(\theta) \qquad [10]$$

where, λ_L is the longitudinal dispersivity of the medium, λ_T is the transversal dispersivity of the medium, δ_{ij} is Kronecker delta, (i.e., $\delta_{ij} = 1$ if $i = j$ and $\delta_{ij} = 0$ if $i \neq j$) V_i is the i-th component of the average interstitial solution velocity V, and $D_p(\theta)$ is the soil diffusion coefficient as defined by Bresler (1973a).

By substituting D_{ij} of [10] into [8] and considering only two space dimensions $x_1 = x$ and $x_3 = z$, as in [9] the salt flow equation becomes

$$\frac{\partial(c\theta)}{\partial t} = \frac{\partial}{\partial x}\left(D_{xx}\frac{\partial c}{\partial x} + D_{xz}\frac{\partial c}{\partial z} - q_x c\right) + \frac{\partial}{\partial z}\left(D_{zz}\frac{\partial c}{\partial z} + D_{zx}\frac{\partial c}{\partial x} - q_z c\right) \quad [11]$$

where the subscripts x and z denoting the direction x_1 and x_3, respectively and D_{xx}, $D_{xz} = D_{zx}$, and D_{zz} are given in [10]. Note that equation [8] and [11] do not include sinks or sources due to uptake by plants or precipitation, dissolution and adsorption of solute. Note also that in the development of [8] and [11], one usually assumes that the soil is a stable, isotropic and homogeneous porous medium, that Darcy's law applies in both the saturated and the unsaturated zones, and that the solute transport is governed by convection and diffusion.

Water flow boundary conditions

Referring to Figure 1, we shall place the origin (0,0,0) of the coordinates at the center of a particular emitter (trickle source, TS), and define W as the domain $W = \{0 \le x \le X,\ 0 \le y \le Y,\ 0 \le z \le Z\}$. It is clear that $x = 0$, $x = X$, $y = 0$, and $y = Y$ are planes of symmetry, for which the normal derivative of θ must vanish, and there is no flow across these boundaries. If one also assumes that $\partial\theta/\partial z = 0$ at the depth $z = Z$ is a good approximation for the period of the infiltration, or at least that imposing this condition would have a negligible effect on the region of interest, one has the following boundary conditions for $\theta(x,y,z,t)$:

$$\partial\theta/\partial x = 0 \quad \text{at } x = 0 \quad \text{and } x = X \text{ for } t > 0$$
$$\partial\theta/\partial y = 0 \quad \text{at } y = 0 \quad \text{and } y = Y \text{ for } t > 0 \qquad [12]$$
$$\partial\theta/\partial z = 0 \quad \text{at } z = Z \text{ for } t > 0$$

In order to define the boundary conditions at the soil surface ($z = 0$), two additional assumptions must be made. First, discharge from the trickle source is known as a function of time. This rate of discharge is denoted by $f(t)$ and will be referred to as trickle discharge. The second assumption refers to the horizontal area across which infiltration takes place. It has been observed that in general a radial area of ponded water develops in the vicinity of the trickle source. This area is initially very small, but its radius becomes larger as time increases. Since the ponded body of water is usually very thin, one can safely neglect the effect of storage of water at the soil surface. This means that the water from the trickle source is able to infiltrate into the soil, or evaporate into the air, instantaneously. Obviously, the soil water content immediately beneath the ponded area is always equal to the water content at saturation, θ_s. Since this saturated area is the only place where water can infiltrate into the soil element, W, we shall refer to it as the saturated area, or the zone of water entry. It is assumed that the center of this disk-like zone is at (0,0,0) and that its radius $\rho(t)$ is a function of time. The only additional boundary condition that must be satisfied at the soil surface outside the saturated area of water entry is that the water flux be equal to a given rate of evaporation, E.

Therefore, the boundary conditions that must be satisfied at the soil surface are conditions of moving boundary. Thus, for all $t > 0$ we have at $z = 0$ the conditions,

$$\theta = \theta_s \qquad \text{for } 0 \le x^2 + y^2 \le [\rho(t)]^2 \qquad [13]$$

$$K(\theta) + E - K(\theta)\frac{\partial p}{\partial z} = 0 \text{ for} \qquad x^2 + y^2 > [\rho(t)]^2 \qquad [14]$$

$$\iint_G [K(\theta_s) + E - K(\theta_s)\frac{\partial p}{\partial z}]\, dx\, dy = \frac{1}{4} f(t) \qquad [15]$$

where G is the quarter disk defined by

$$x^2 + y^2 \le [\rho(t)]^2; \quad x,y > 0,$$

and θ_s is the water content of saturated soil, $\rho(t)$ is the radius of the ponded or water saturated area (cm), $E = E(\theta,t)$ is a given evaporation func- ($cm^3\ cm^{-2}\ min^{-1}$), and $f(t)$ is the trickle source discharge (cm^3/min).

We have thus confined our flow problem to the cube,

$$W = \{0 \le x \le X,\ 0 \le y \le Y,\ 0 \le z \le Z\}$$

on the sides of which we were able to formulate suitable boundary conditions. To these we have to add the initial conditions

$$\theta = \theta_n \text{ in } W, \text{ for } t = 0 \qquad [16]$$

where θ_n is the initial soil water content.

At present, the problem defined in equations [7] and [12] through [16] can be solved only by numerical methods with the aid of a computer. Large amounts of computer time are needed in order to solve the four-dimensional grid (x,y,z,t) in this kind of problem. As a first approach, we restrict our-

selves to two-space dimensional problems where the computer time required is greatly reduced. Also two-dimensional experimental data for comparison are more easily obtained. Such two-dimensional flow is the cylindrical flow which takes place in the field as long as the wetting has not reached the outer boundaries of the volume element W. Other cases of a two-dimensional problem are: (a) a line of trickle sources very close to one another, and (b) a line of perforated or porous tube. Here, the problem can be viewed essentially as one of plane flow. Thus, two mathematical models will be investigated in the present study: (1) a "plane flow" model involving the Cartesian coordinates x and z, and (2) a "cylinder flow" model described by the cylindrical coordinates r and z.

Axisymetric-cylindrical flow models

In the axisymetric cylindrical flow model the case of a single trickle nozzle (or a number of nozzles spaced at sufficient distance apart) is considered. The origin is at the center of the emitter and c and θ are functions of the coordinates $z = x_3$, t, and $r = (x^2 + y^2)^{1/2} = (x_1^2 + x_2^2)^{1/2}$. Due to the radial symmetry conditions and considering the aforementioned assumptions, eqs. [7] and [8] take the form

$$\frac{\partial\theta}{\partial t} = \frac{\partial}{\partial r}\left[K(\theta)\frac{\partial p}{\partial r}\right] + \frac{K(\theta)}{r}\frac{\partial p}{\partial r} + \frac{\partial}{\partial z}\left[K(\theta)\frac{\partial H}{\partial z}\right] \qquad [17]$$

$$\frac{\partial(c\theta)}{\partial t} = \frac{\partial}{\partial r}\left(D_{rz}\frac{\partial c}{\partial z} + D_{rr}\frac{\partial c}{\partial r}\right) + \frac{1}{r}\left(D_{rz}\frac{\partial c}{\partial z} + D_{rr}\frac{\partial c}{\partial r}\right) + \frac{\partial}{\partial z}\left(D_{rz}\frac{\partial c}{\partial r} + D_{zz}\frac{\partial c}{\partial z}\right)$$

$$- \left[\frac{\partial(q_z c)}{\partial z} + \frac{\partial(q_r c)}{\partial r} + \frac{q_r c}{r}\right] \qquad [18]$$

The initial and boundary conditions for $\theta(x,r,t)$, (eq. [17]) in the cylindrical element $W = (0 \le r \le R,\ 0 \le z \le Z)$ are as follows:

$$\theta = \theta_n;\ 0 \le r \le R;\ 0 \le z \le Z;\ t = 0 \qquad [19a]$$

$$\frac{\partial\theta}{\partial r} = 0;\ r = 0,\ r = R;\ 0 \le z \le Z;\ 0 \le t \le T \qquad [19b]$$

$$\frac{\partial\theta}{\partial z} = 0;\ 0 \le r \le R;\ z = Z;\ 0 \le t \le T \qquad [19c]$$

$$\theta = \theta_s;\ 0 \le r \le \rho(t);\ z = 0;\ 0 \le t \le T \qquad [19d]$$

$$E - K(\theta_s)\frac{\partial H}{\partial z} = 0;\ \rho(t) < r \le R;\ z = 0;\ 0 \le t \le T \qquad [19e]$$

$$2\pi \int_0^{\rho(t)} [E - K(\theta_s)\frac{\partial H}{\partial z}] r dr = f(t) \qquad [19f]$$

where T is the end time of infiltration.

The boundary and initial conditions for $c(r,z,t)$, (eq. [18]) under the axisymetric flow conditions of infiltration from trickle sources are

$$\frac{\partial c}{\partial r} = 0 \text{ at } r = 0 \text{ and } r = R \text{ for } t > 0 \qquad [20a]$$

$$\frac{\partial c}{\partial z} = 0 \text{ at } z = Z \text{ for } t > 0 \qquad [20b]$$

and at $z = 0$ for $t > 0$:

$$-[D_{rz}(r,0,t)\frac{\partial c}{\partial r} + D_{zz}(r,0,t)\frac{\partial c}{\partial z}] + q_z(r,0,t)\ c(r,0,t) = 0$$

$$\text{for } \rho(t) \le r \le R \qquad [20c]$$

$$-[D_{rz}(r,0,t)\,\frac{\partial c}{\partial r} + D_{zz}(r,0,t)\,\frac{\partial c}{\partial z}] + q_z(r,0,t)\;c(r,0,t) =$$

$$q_z(r,0,t)\;C_o(t) \qquad \text{for } 0 \le r \le [\rho(t)] \qquad [20d]$$

or in analogy with the boundary condition [19d] and [19f] equation [20d] may be replaced by

$$c(r,z = 0,\; t > 0) = C_o(t) \text{ for } 0 \le r \le [\rho(t)] \qquad [20e]$$

$$2\pi \int_0^{\rho(t)} \{-[D_{rz}(r,0,t)\,\frac{\partial c}{\partial r} + D_{zz}(r,0,t)\,\frac{\partial c}{\partial z}] + q_z(r,0,t)\;c(r,0,t)rdr = f(t)C_o(t) \qquad [20f]$$

and finally the initial conditions are

$$c(r,z,0) = c_n(r,z) \text{ in } W \text{ for } t = 0 \qquad [20g]$$

Here, $q_z(r,0,t)$ is the specific downward flux of water at the soil surface as given by Darcy's law, C_o is the solute concentration at the inlet of the trickling water, $c_n(r,z)$ is the predetermined initial soil solution concentration, and $D_{rz}(r,0,t)$, $D_{zz}(r,0,t)$ are the hydrodynamic dispersion coefficients at the soil surface, the sum of diffusion and mechanical dispersion coefficients as given by [10].

Plane flow model

Consider: (a) An infinite straight line of perforated or porous tube, or (b) a set of drippers that are spaced very close to each other at equal intervals along an infinite straight line, so that their ponding areas overlap after only a short period of time. One can assume that the total ponding area has the form of an infinite strip of width $\rho(t)$. Let this strip be oriented along the y axis, and let x be the horizontal coordinate normal to

y. The flow becomes independent of the y coordinate. Considering plane flow model the governing equations [9] and [11] are now applied. Note also that the variable y must now be eliminated from the boundary conditions [12] through [16], and that x is substituted for r and X for R in [20] and that 2π and r in the last term on the LHS of [20f] must also be omitted. Note also that f(t) is now the trickle discharge per unit length of the strip ($cm^3\ cm^{-1}\ min^{-1}$).

This plane flow model is relatively easy to reproduce in the laboratory and can therefore serve as a convenient tool for comparison purposes. Such a comparison between laboratory and theoretical results will be described in detail in a subsequent section.

Solutions

The problems defined by the nonlinear partial differential equations [17] and [18] or [9] and [11] together with the associated boundary conditions [19] and [20] can, at present, be solved only by numerical methods with the aid of a computer. Brandt et al. (1971) used an approach that combined the non-iterative alternating-direction implicit (ADI) difference method with the iterative Newton's method to solve numerically for the value of $\theta(r,z,t)$, $q_r(r,z,t)$ and $q_z(r,z,t)$. The calculated values can then be used to obtain $c(r,z,t)$ from [18]. To solve for $c(r,z,t)$ by the second-order finite difference approximation to [18] or [11] and [20], (Bresler, 1975), the values of $D_{rr}(r,z,t)$, $D_{rz}(r,z,t)$, and $D_{zz}(r,z,t)$ must be known. Since $\theta(r,z,t)$ and $q(r,z,t)$ are now known, one calculates $V_r(r,z,t) = q_r(r,z,t)/\theta(r,z,t)$ as well as $V_z(r,z,t) = q_z(r,z,t)$ and $V = (V_z^2 + V_r^2)^{1/2}$; and estimates D_{zz}, D_{zr}, and D_{rr} from [10]. The methods used to solve for $\theta(r,z,t)$ (Brandt et al., 1971) and $c(r,z,t)$ (Bresler, 1975) resulted in a numerical technique that is simple, efficient, unconditioned stable and second-order accurate.

Comparison with experimental data

The solution of the aforementioned mathematical models by the numerical technique attached to it must be compared with experimental results in order to establish the reliability of the theoretical models, to evaluate the physical assumptions involved in them, and to ascertain the validity of the views expressed in the theories. Laboratory experiments were conducted under conditions similar to those assumed in the two-dimensional plane flow models with $y << x$ so that $y \to 0$ was practically correct (Bresler et al., 1971; Bresler and Russo, 1975).

Quantitative comparisons between the theoretical and experimental water content results are given in Fig. 2 where the water content profiles in the z dimensions are shown. This figure shows several sets of experimental data for each constant value of discharge together with the corresponding theoretical continuous curves. The theoretical results are calculated by the numerical method of Brandt et al. (1971) with the aid of soil water parameters $K(\theta)$ and $D(\theta)$ of Gilat loam soil (Bresler et al., 1971).

The comparison between the calculated and experimental data was made for all times and points for which there were water content determinations, and at all the tested rates. In order to facilitate the comparison, the moisture content was plotted as a function of the distance for the single z space coordinate. In Fig. 2 we present the water content distribution along the center vertical plane $[\theta(0,z)]$ for five different measurement times (t) and at four rates (Q). Note that the zero point ($z = 0$) was shifted and the data were accordingly translated along the z axis, in order to distinguish between the different sets. The shifting of the data provides easier identification of the experimental points which corresponded to the calculated

lines, Note also that due to the plane geometry f(t) = Q is given as L^2T^{-1} (cm^3 cm^{-1} min^{-1}). From Figure 2 it can be seen that the agreement between the calculated and the measured water content distribution is generally quite good.

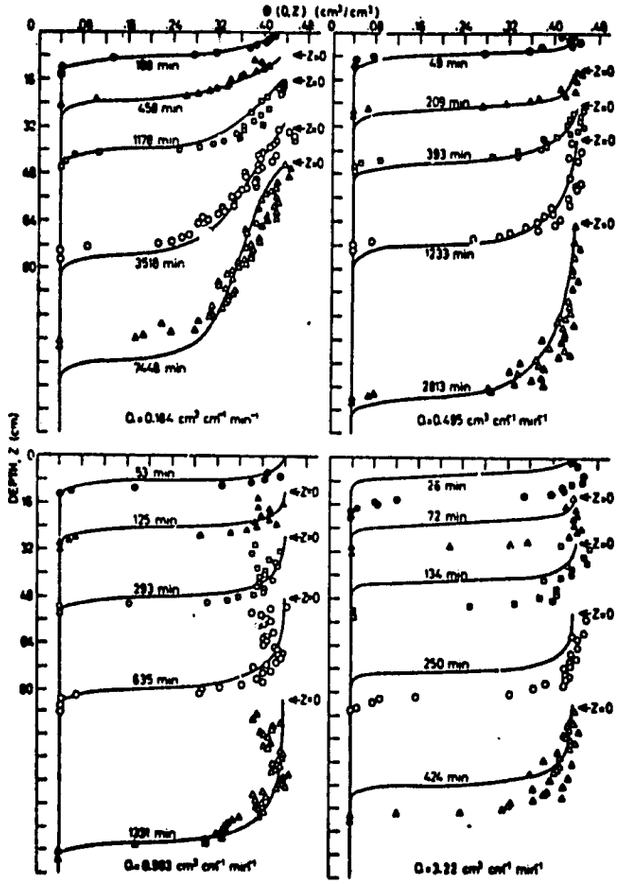

Figure 2. Vertical water content distribution, (0,z), in the plane of symmetry (x = 0). Computed results (solid lines) are compared with experimental data of Gilat loam soil (scattered points). The numbers labeling the lines indicate infiltration time (t); Q indicates the discharge per unit length. (After Bresler et al., 1971).

In the case of infiltration into an air-dry soil, a clear boundary exists between the wetted zone and the dry zone in the wetting front. The wetting front is easy to determine experimentally with a minimum error. If this wetting front can also be detected by the results of the numerical calculation, the location of the front could serve as a good indicator for comparing calculated and experimental results. Furthermore, the wetting front may be important from a practical point of view since it shows the boundaries of the irrigated soil volume.

In the laboratory experiment with the initially air-dry Gilat soil, it was easy to visually identify the wetting front through the perspex plates. For comparison, the location of the wetting front in the corresponding numerical solution was defined as a ridge (or line of maxima) of $|\text{grad}\ \theta|$.

Figure 3 shows a comparison between the location of the calculated wetting front and the observed one, as a function of the space coordinates (x,z) and the total infiltration time. The total infiltration time is indicated on each wetting front line that appears in the figure. As in the case of soil moisture distribution (Fig. 2), the agreement between the experimental wetting front and the calculated one is good.

A comparison between the location of the computed wetting front and its observed position (Fig. 3) and between calculated and measured θ (Fig. 2) may serve as an indicator for the ability of the model to predict water flow. The fact that the agreement between calculated and observed water content distribution (Fig. 2) and wetting front (Fig. 3) is generally good suggests that model computations of water flow have little effect on discrepancies or agreements between measured and computed salt flow data (Fig. 4).

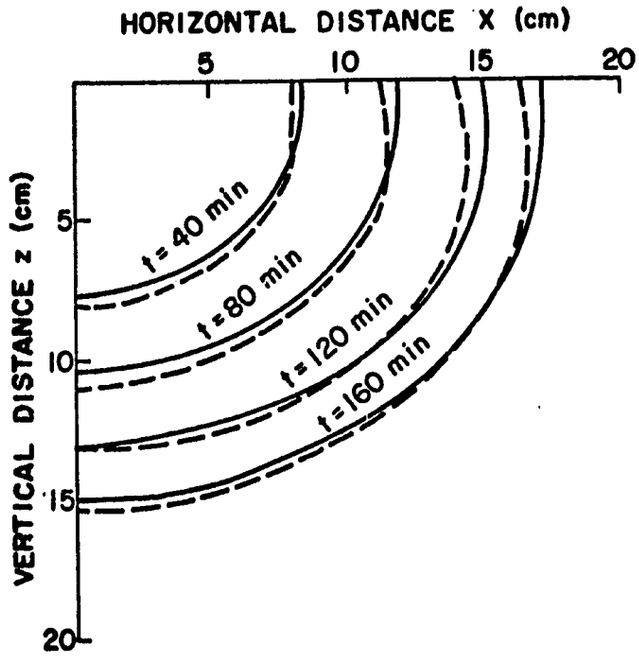

Figure 3. Computed wetting front position (solid lines) as compared with the observed one (dashed lines) for four infiltration times (the number labeling the lines). (after Bresler and Russo, 1975)

The comparison between measured chloride concentration and computed solute distribution data after 160 minutes of infiltration are given in Figure 4 (Bresler and Russo, 1975). To be consistent with Figure 9 the salt distribution data are expressed in a dimensionless relative form, $(c - C_o)/c_n$, where c and c_n are the concentration in the soil solution

at t = T and t = 0, respectively, and C_o is inlet concentration. In order to facilitate the comparison the salt data in Figure 4 are also shifted along z. In Figure 4 we present the data along the vertical axis (z) at five different horizontal distances from the source: x = 0, 3, 7, 11, and 15 cm., i.e. c(0,z), c(3,z), c(7,z), c(11,z), and c(15,z). Note that here also the zero point (z = 0) was shifted and the data were accordingly translated along the z axis in order to distinguish between the different sets. The agreement between theoretical and measured salt distribution results is clearly observed in Figure 4.

The agreement between laboratory and numerical salt flow results, which is as good as one could expect for our simple laboratory technique (Bresler and Russo, 1975), shows that two-dimensional transport of solute during nonsteady infiltration may be almost quantitatively predicted by the theoretical model (Bresler, 1975). However, the prediction capability of the model and its applicability may be restricted to the conditions which prevailed in the experiment. For example, it may not be applicable for conditions of fingering induced by spatial density variation in the mobile phase. Furthermore, it may be limited to predicting salt transport only if the dispersion tensor D_{ij} depends on the flow pattern as described by [10]. The data of Figure 4 suggest that these restrictions do not occur under the experimental conditions. Yet, the experimental data from a single laboratory study might be insufficient for general detailed model verification.

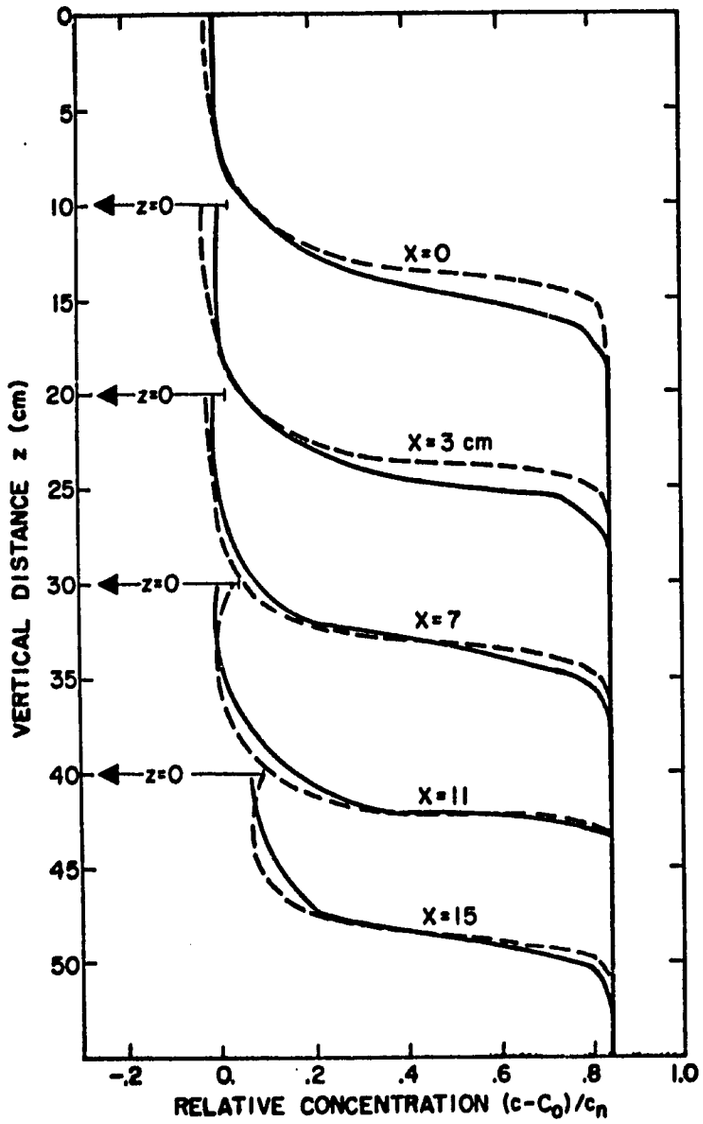

Figure 4. Vertical salt concentration distribution in terms of $(c-C_o)/c_n$ in 5 horizontal planes. Computed "plane flow" results (solid lines) are compared with measured chloride data (dashed lines). Note that the zero vertical plane (z = 0) is shifted and the data are accordingly translated along z axis. (after Bresler and Russo, 1975).

SOIL WATER REGIME DURING TRICKLE INFILTRATION

The effect of any irrigation method on the soil-water regime depends primarily on the conditions prevailing at soil-surface boundary. In the case of trickle irrigation, these conditions may be defined by the trickle discharge (Q) measured as the amount of water per unit time, by the horizontal area across which infiltration takes place ($A = \pi\rho^2$) and by the rate of evaporation at the soil surface (E). The last factor becomes important only when the potential evaporation is extremely high and the saturated hydraulic conductivity of the soil is very low.

As already mentioned, it was observed that, in general, a radial area of ponded water develops in the vicinity of the trickle source. This area is initially very small, but its radius becomes larger with time. Water from the trickle is able to infiltrate through this area into the soil, or evaporate from it into the air, instantaneously. Obviously the soil-water content immediately beneath the ponded area, $A = \pi\rho^2$, is always equal to the water content at saturation, θ_s. The size of this saturated area is a function of time and is the only place where water can infiltrate into the soil from the surface. Thus, the rate at which water enters the soil across this area is equal to the rate of trickle discharge, minus the rate of evaporation.

Figure 5 shows the calculated vertical water flux at the surface across the saturated water entry zone, as a function of infiltration time and distance from the center of source. Since $\theta = \theta_s$ in the interval $0 \leq r \leq \rho(t)$, the hydraulic conductivity of the saturated zone is constant

(K saturated). Thus, the decrease in water flux with time (Figure 5) is due only to the decrease in the vertical hydraulic gradient at the surface. Within the time considered, the hydraulic gradient is always less than unity.

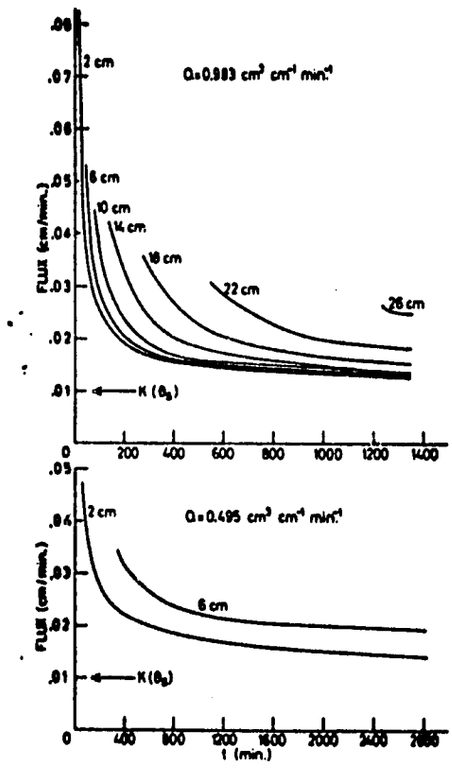

Figure 5. Computed vertical surface water flux in the saturated zone as a function of time (t) and horizontal distance (r) from the source for two cases of trickle discharge (Q) (after Brandt et al., 1971).

The larger the trickle discharge and the smaller the distance from the source, the faster the hydraulic gradient as a function of time approaches a limit. If this limit were one, then $q = k(\theta_s)$, but it is clear from Figure 5 that this has actually not happened. If a limit of one were approached throughout the ponded area, the we would have from eq. [19f] $\rho(t \to \infty) \to [Q/K(\theta_s)\pi]^{1/2}$. At any rate for any finite value of time, $\rho(t) < (Q/\pi K_{sat})^{1/2}$ in cylindrical flow ($\rho(t) < Q/(2K_{sat})$ in plane flow). If evaporation is too significant to be neglected, then, of course $\rho(t) < \{Q/[K_{sat} + E)]\}^{1/2}$. Neglecting evaporation the difference between $\rho(t)$ and $[Q/(K_s\pi)]^{1/2}$ (or $Q/(2K_{sat})$) depends on the average surface water pressure gradient over the interval $0 \leq r \leq \rho(t)$. Since the rate of change of this average value decreases with time, the rate of growth of the saturated water entry zone also decreases with time, as shown in Figure 6. This figure further indicates that at the end of the infiltration process $\rho(T) < Q/(2K_s)$.

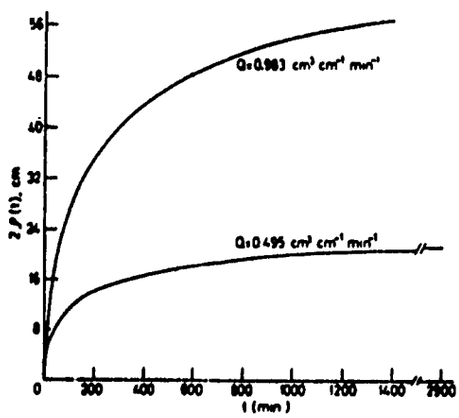

Figure 6. Saturated water entry distance [2 (t)] as a function of infiltration time (t) for two trickle discharges. (Q). (after Brandt et al., 1971).

To illustrate the water-content distribution, the plane flow model is considered. Examples of water-content distribution for two cases of trickle discharge (Q), expressed in terms of discharge per unit length are given in Figure 7, which shows how the soil water content changes with time and position during trickle infiltration. The illustration also shows the effect of trickle discharge on the water content field. The saturated water-entry area (A), and the rate at which it changes with time, are shown by the particular line of saturated water content at the surface, where $\theta_s = 0.44$. In general, this area increases as the rate of trickle discharge increases. In the vicinity of the source ($x = 0$, $z = 0$ in Figure 7), the moisture gradients increase when the rate of discharge decreases. These gradients can be calculated from the distances between lines of equal water content. This condition reverses as the wetting front is approached. The overall shape of the wetted zone also depends on the trickle discharge. The vertical component of the wetted zone becomes larger and the horizontal component narrower as the rate of discharge decreases.

In the case of infiltration into a dry soil, a distinct boundary exists between the wetted zone and the dry zone; this is known as the wetting front. The wetting front is important in trickle infiltration because it indicates the boundaries of the irrigated soil volume. Figure 8 shows the location of the wetting front, as a function of the space coordinates (x,z) and the total amount of infiltrated water, for 4 different trickle discharges. The total amount of infiltrated water (in liters) is indicated on the wetting front lines appearing in the figure. The trickle discharge, in terms of rate per unit length Q, is also indicated.

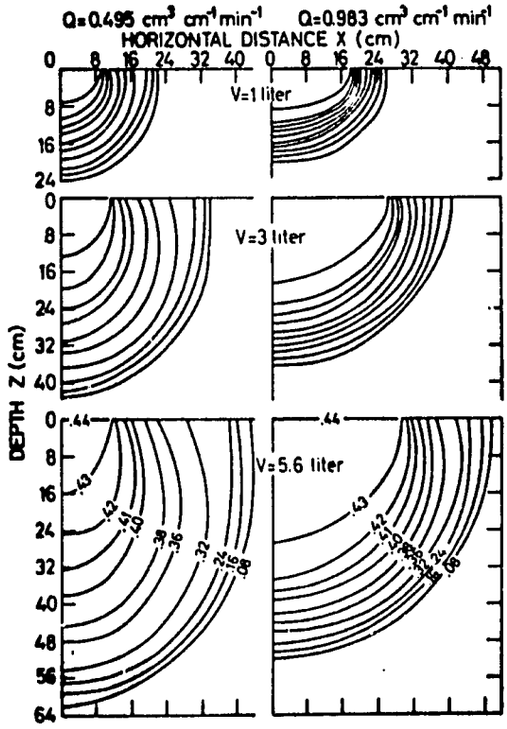

Figure 7. Water-content field as a function of cumulative infiltration (V) for two cases of discharge (Q). The number labeling the curves indicate water content (θ). (after Brandt et al., 1971)

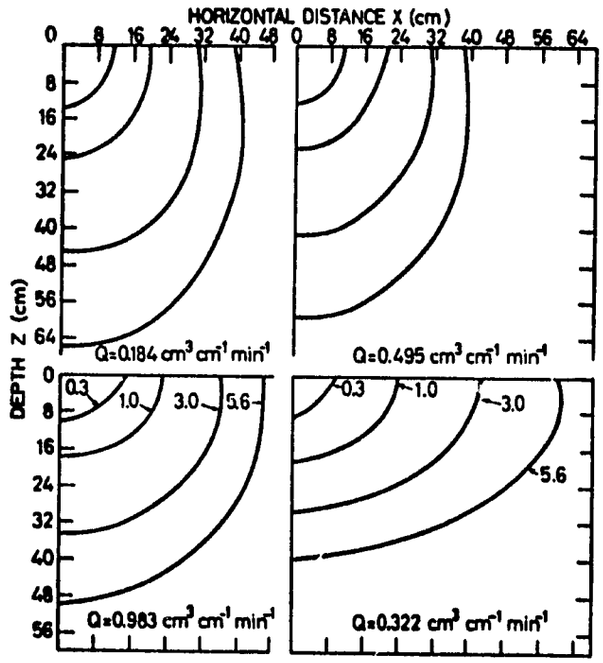

Figure 8. Wetting front position as a function of infiltration time and discharge (Q). The number labeling the lines indicates cumulative infiltration water (in liters). (after Bresler et al., 1971).

The data presented in Figures 7 and 8 clearly demonstrate that the rate of trickle discharge has a remarkable effect on the shape of the wetted soil zone. Increasing this rate results in an increase in the horizontal wetted area and a decrease in the wetted soil depth. This is probably due to a change in the size of the water-entry saturated zone for each rate of discharge (Figures 6 and 7), the latter zone becomes larger as the trickle

rate increases.

The possibility of controlling soil-water content, suction, fluxes, and the wetted volume of the soil by regulating the trickle discharge (Figures 5 and 8), is of practical interest in the design of field irrigation systems (see later).

A possible effect of soil water evaporation, which occurs simultaneously with infiltration, on the water distribution pattern was also tested by the numerical technique of Brandt et al. (1971). For this scheme, evaporation flux as a function of soil water content must be known. Such a function $E(\theta)$, was constructed by calculating evaporation of water from the top 30-cm soil layer using the numerical procedure of Hanks, Klute and Bresler (1969). The results of water distribution data, using a high potential evaporation value of E_o = 10 mm/day, remain essentially the same as if evaporation were completely neglected. It appears, therefore, that generally water evaporation which takes place during infiltration, is not an important factor in infiltration from a trickle source. This is so because generally free water evaporation (E_o) rate is less than 1 cm day^{-1} and K_s of many "normal" soils is in the order of 1 cm hour^{-1} so that E_o/K is generally about 0.04. The net water flux into the soil anywhere in the saturated water entry zone is given by $q_{net} = -K_s \text{ grad } H - E_o$. Since grad H during infiltration is always negative then the ratio between outward flow to inward flow is $E_o/(-K_s \text{ grad } H) < 0.04$. However in cases where E_o is extremely high and K_s is extremely low the effect of evaporation during infiltration from a trickle source may be important.

SOLUTE DISTRIBUTION DURING INFILTRATION

As mentioned before the accumulation of salt between emitters may be a serious problem for crops irrigated by trickling. Control of soil salinity regime is therefore essential to the permanent operation of a trickle irrigation system. In addition, since fertilization simultaneously with irrigation seems to be a good practice, optimizing of the nutritional regime in the root zone depends on the possibility of controlling the fertilizer salts in the irrigated soil. Salt distribution in the soil under trickle irrigation will be demonstrated in this section by a few typical examples. From these examples one can evaluate the applicability of the method to the control of soil salinity and fertility by tricklers under various conditions. The controlled leaching process involves the case of inflow with low concentration that miscibly displaces a highly concentrated soil solution originally present in the porous medium. In this discussion interactions between the solute and the soil matrix are ignored. Two soil media with widely different hydraulic properties and salt dispersion characteristics were investigated.

The results presented in Figures 9 and 10 were obtained from the cylindrical flow model when the hydraulic soil functions $K(\theta)$ and $p(\theta)$ were those of Gilat (loam) and Nahal Sinai (sand) soils (for details, see Figures 1, 2, 3 in Bresler et al., 1971). The soil diffusion coefficient was taken as $D_p(\theta) = 0.004 \exp(10\theta)$, and the dispersivities were chosen to be $\lambda_L = 0.2$ cm, and $\lambda_T = 0.01$ cm (Perkins and Johnston, 1963). The soils are assumed to have initially uniform water and salt contents. Calculations were performed by using an initial water content and salt concentration of $c_n(r,z) = 52.35$ meq/liter and $\theta_n(r,z) = 0.213$ for Gilat; $c_n(r,z) = 300$ meq/liter

and $\theta_n(r,z) = 0.0375$ for Nahal Sinai; with $\theta_s = 0.265$ and $\theta_s = 0.44$ for Nahal Sinai and Gilat, respectively. Note that the initial water content values are in the "available" moisture range for both soils. Note also that the "water capacity" ($\theta_s - \theta_n = 0.227$) and the initial volumetric salt content ($c_n\theta_n = 11.25$ meq/liter soil) are the same for the two soils investigated. The values of $C_o\theta_s$, which is the minimum possible volumetric salt content at the soil inlet, was also the same for the two soils, i.e. inlet salt concentration of $C_o(t) =$ 5 meq/liter for Nahal Sinai and $C_o(t) = 3.0$ meq/liter for Gilat soil. Two cases of trickle discharge, $f_1(t) = Q_1 = 4$ liter/hr and $f_2(t) = Q_2 = 20$ liter/hr are considered which assumed to remain constant throughout the infiltration period.

The general pattern of salt distribution in the two soils studied and for the two trickle discharges, is demonstrated in Figures 9 and 10. In Figure 9 the salt distribution field is expressed in terms of salt concentration in the soil solution (as meq solutes/liter soil solution), or in a dimensionless relative form (as $(c - C_o)/c_n$). Figure 10 presents the salt content field data in terms of salt content per unit bulk volume of the soil (as meq/liter bulk soil). Both figures show how the position of the dissolved salt field in the cylindrical flow is influenced by the trickle discharge and the hydraulic conductivities of the two soils (Bresler et al., 1971) during infiltration. The location of the wetting front and the radius (ρ) of the saturated water entry ponding zone are also given (the heavy solid lines in Figures 9 and 10). The size of the water entry zone and the location of the wetting front are very important from a practical point of view, since they are indicators of the boundaries of the wetted soil volume.

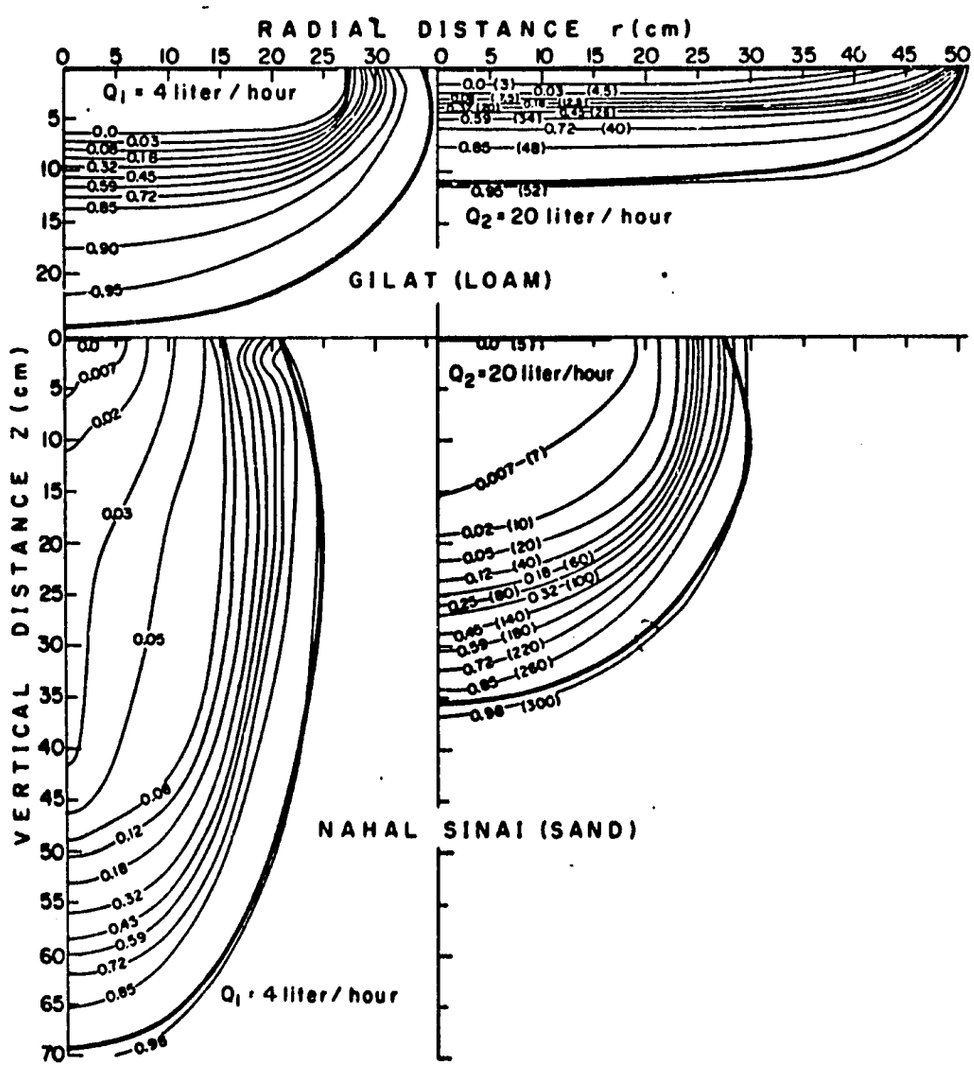

Figure 9. Computed salt concentration field for two cases of trickle discharges (Q_1 and Q_2) and two soils (Gilat - loam and Nahal Sinai - sand). The numbers labeling the curves indicate relative concentration in terms of $(c - C_o)/c_n$. The numbers in parenthesis are salt concentrations (c), in meq/liter soil solution. The upper heavy solid lines indicate the saturated water entry radius, (ρ) and the peripheral heavy lines are the wetting fronts.

The fact that the water capacity ($\theta_s - \theta_n$), the initial volumetric salt content ($c_n\theta_n$) and the minimum inlet salt content ($C_o\theta_s$) are identical in the two soils, makes it possible to compare the salt distribution data (Figures 9 and 10) of these two soils. In addition, in order to be able to compare the effect of trickle discharges and to place the two different rates on an equal basis, the results are compared for an identical amount of cumulative infiltration (12 liters) and not for an equal time allowed for the infiltration. It should be noted that most of the initial and boundary data, such as θ_s, θ_n, c_n, C_o, Q and total infiltration used in the examples, are in the practical and actual field conditions' range.

Figure 9 demonstrates the effect of trickle discharge and soil hydraulic properties on the shape of the actual salt concentration distribution. In both soils and trickle discharges, the solution concentration of the saturated water entry zone is identical to that of the infiltrated water. The concentration rises as the wetting front is approached and reaches its initial value near the wetting front boundary. It is clear that the shape of the overall wetted zone, which lies between the heavy lines (Figures 9 and 10), is soil- and discharge-dependent. Therefore, the salt distribution pattern should also be affected by these properties. Thus, the completely leached zone, $(c-C_o)/c_n = 0$, remains at the water-saturated zone in the sandy soil but it penetrates to a certain depth in the loam soil. In addition, the leached part of the soil in the vertical component of the wetted zone is deeper, and in the radial component is narrower, as the soil becomes coarser (having higher hydraulic conductivities) and as the trickle discharge becomes slower.

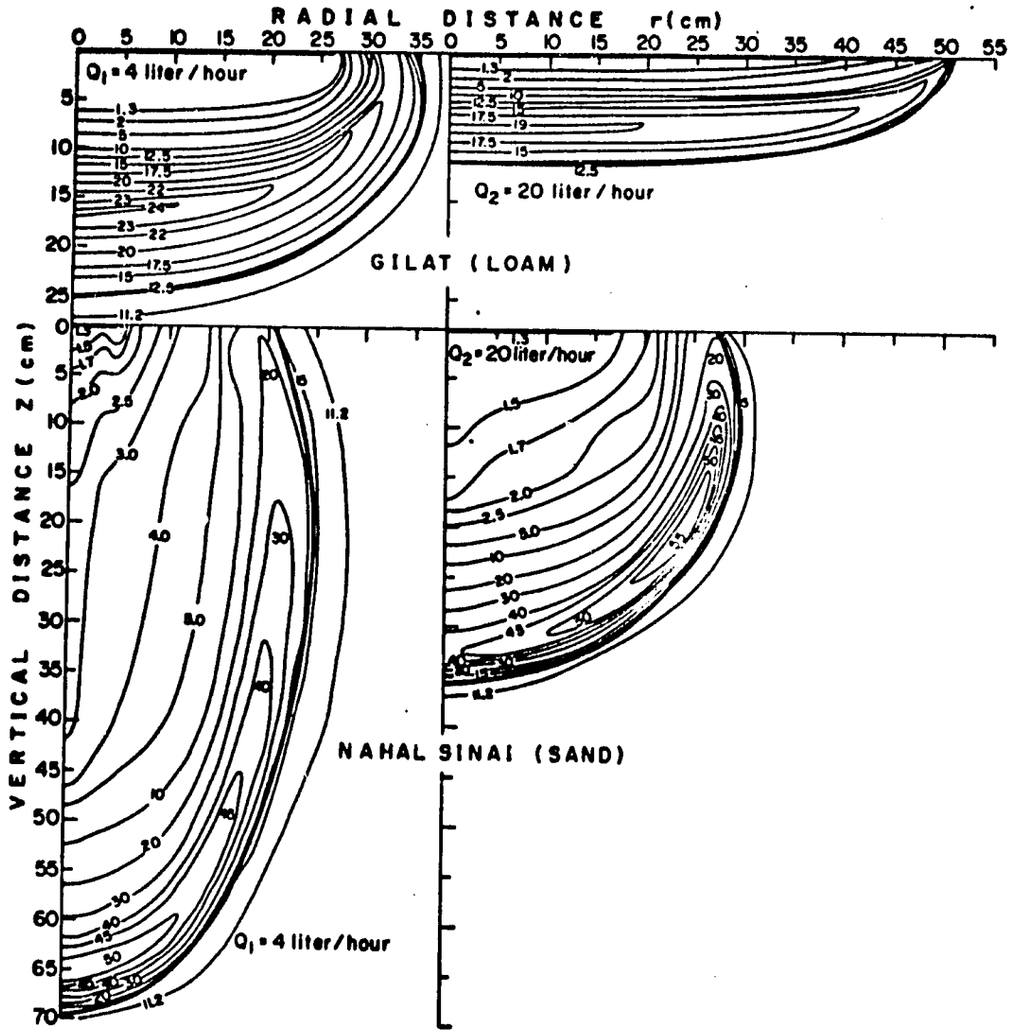

Figure 10. Computed volumetric salt content field ($c\theta$) for two cases of trickle discharges (Q_1 and Q_2) and two soils (Gilat and Nahal Sinai). The numbers labeling the curves indicate volumetric salt content ($c\theta$) in meq/liter bulk soil. Heavy solid lines indicate the same as in Figure 9.

The picture for the volumetric salt content field (Figure 10) differs from that of Figure 9 owing to the fact that the salt content pattern is affected by the distribution of both water content (θ) and salt concentration (c). Thus, although the pattern of the leached part, close to the saturated zone, is similar in Figure 10 to that of Figure 9, the accumulation part--close to the wetting front--is completely different. Here (Figure 10) the salt quantities from the leached part of the soil are accumulated and reach a maximum at a certain distance from the source. As is demonstrated in Figure 10, the location of this maximum salt accumulation zone is largely dependent on both soil hydraulic properties and the discharge rate of the trickle. The size of this maximum salt content, however, is affected mainly by the soil properties and not by the discharge rate.

The general pattern of salt distribution and its dependence on initial salinity, salinity of the inlet water, rate of trickle discharge, and the hydraulic characteristics of the soil, as demonstrated in Figures 9 and 10, is of practical interest for problems connected with the design of a field irrigation system, in order to control the soil salinity or fertility in the wetted root zone. Consider, for instance, an initially saline field being irrigated by a set of symmetrical emmiters sufficiently far apart. Suppose that it is important to evaluate the leaching effectiveness of removing salts from a given root volume in which the main plant roots function. With an infiltration duration large enough, depending on soil and discharge rate, this leached zone may be sufficient for most of the roots to concentrate and function without disturbance. On the other hand, a large quantity of salt may accumulate to an appreciable level at a certain distance from the source close to the wetting fronts (Figure 10). It is apparent (Figure 10) that one

can overcome this limitation to plant growth by changing the discharge of the source, its position, or both.

Applications of the data of Figure 10 to fertilization problems are possible. In this case the complete leached zone $(c - C_o)/C_n = 0$ may be interpreted as the part of the root zone in which the concentration of the nutrient in the soil solution is identical to its concentration in the irrigation water. Knowing this region is of practical importance from a point of view of efficient use of fertilizers.

APPLICATION OF INFILTRATION MODELS TO THE DESIGN OF TRICKLE IRRIGATION SYSTEMS

In the previous chapters a specific model of transient infiltration from trickle sources has been discussed. From this model the pattern of two-dimensional soil-water distribution can be obtained for soils with various hydraulic properties and for different trickle discharges. It has also been shown that the actual water source does not behave as an idealized point source but the water is spaced over a finite circular water saturated area on the soil surface. This radial saturated water entry zone is initially very small but its radius becomes larger as time increases and approaches a constant value at some finite infiltration time. The ultimate size of this zone depends primarily on the saturated hydraulic conductivity of the soil and the discharge rate of the dripper.

The case of steady infiltration from a shallow circular ponded area on the horizontal surface of a semi-infinite soil was treated by Wooding (1968) using the method of linearization proposed by Philip (1968). The conditions of steady infiltration may be met when irrigation is continuous for a relatively long time, and in intermittent irrigation when irrigation frequency is of the order of one day or less. When irrigation is very frequent water content pulses resulting from intermittent infiltration are dumped out few centimeters from the source for most soils (Rawlins, 1973). This makes it possible to consider flow beyond this region to be essentially steady especially since infiltration period is long compared to the water extraction period. For steady infiltration an estimate of the saturated water entry zone, can be obtained from the analysis of the results of Brandt et al.

(1971). The outcome from this analysis in a combination with Wooding's (1968) solution is a useful tool for the purpose of designing trickle irrigation systems. These are the main objectives of this chapter.

Steady infiltration from a circular pond

As has been stated, it is possible to consider steady state flow, at certain distances from the emitters, for continuous irrigation when infiltration takes place during relatively long time, and for intermittent irrigation when irrigation frequency is of the order of a day or less. Of course, a truly steady-flow can never be achieved during trickle infiltration but it represents an asymtotic case which can be used to generalize the specific flow theory for practical purposes of designing trickle irrigation.

Governing Equation

In practice it is sometimes possible to approximate the nonhysteritic hydraulic conductivity function, K(p), as

$$K(p) = K_s \exp(\alpha p) \qquad [21]$$

where K_s and α are constants characteristic of the soil. Talsma (1963) showed that hydraulic conductivity of some field soils can indeed be represented by eq. [21]. Substituting [21] into [17] and considering steady state flow, the result is a linear differential equation in the form

$$\frac{1}{r}\frac{\partial}{\partial r}\left(r\frac{\partial S}{\partial r}\right) + \frac{\partial^2 S}{\partial z^2} - \alpha\frac{\partial S}{\partial z} = 0 \qquad [22]$$

Here S = S(p) is defined by the transformation

$$S(p) = \int_{p_o}^{p} K(p)dp \qquad [23]$$

where p_o is a reference value defined by $p_o = p(\theta_o)$. The governing equation [22] has been used by Wooding (1968) to solve for steady infiltration from a shallow circular pond.

Boundary Conditions

The boundary conditions appropriate to steady infiltration from a circular source are similar to [19] but consider semi-infinite region with fixed saturated water entry zone (instead of prescribed discharge) and of course, the time variable (t) is excluded. Thus at the soil surface (z = 0) over a constant ponded water entry area, water content is at saturation, or in terms of the transformed variable S(p),

$$z = 0; \qquad 0 \le r \le \rho_u; \qquad S = \int_p^0 K(p)dp = S_s \qquad [24a]$$

where $S_s = S(p = 0)$ is the value of S in saturated soil, and ρ_u is the ultimate radius of the ponded area when steady state infiltration has been reached.

Beyond the water entry zone over the nonwetted area of the soil surface, the vertical water flux is zero if evaporation may be neglected. This means that in this region $K \frac{\partial p}{\partial z} - K = 0$ or $\frac{\partial S}{\partial z} - K = 0$. From [21] it appears that $\alpha = \frac{\partial K/\partial p}{K} = \frac{\partial K}{K \partial p}$ and therefore

$$\int_{p_o}^{p} K dp = \frac{1}{\alpha} \int_{K_o}^{K} dK$$

Integrating the last equation using [23], one gets $S = \frac{K - K_o}{\alpha}$. During steady infiltration from a trickle source most of the soil surface in the region $r \ge \rho_u$ is air dry, or at least at water content sufficiently low, so that $K_o = K(\theta_o)$ is negligible small to give $K = \alpha S$. It follows therefore that approximately

$$\text{at} \quad z = 0; \quad \rho_u \leq r \leq \infty; \quad \frac{\partial S}{\partial z} - \alpha S = 0 \qquad [24b]$$

If one also assumes that at large distances from the source the low initial water content remains constant, one has the following boundary condition

$$z^2 + r^2 \to \infty, \quad S = S_o \qquad [24c]$$

In order to generalize the solution it is convenient to take the radius ρ_u as the length unit and to define dimensionless cylindrical coordinates $\xi = \frac{r}{\rho_u}$ and $\zeta = \frac{z}{\rho_u}$. The boundary conditions [24] can then be written in terms of ξ and ζ as

$$\begin{aligned} &S(\xi,0) = S(\theta_s) && 0 \leq \xi \leq 1 \\ &\frac{\partial S(\xi,0)}{\partial \zeta} = \rho_u \alpha S(\xi,0) && \xi > 1 \\ &S(\xi,\zeta) = S(\theta_o) && \zeta^2 + \xi^2 \to \infty \end{aligned} \qquad [25]$$

The problem given by [22] and [25] was solved by Wooding (1968). He reduced the boundary conditions to a system of dual integral equations and solved it by a modification of Teauter's (1951) method. His solution is restricted to values of $\alpha\rho_u < 10$, which are sufficiently good for all purposes of practical application of the theory. For example, for $\alpha = 0.1$ the value of ρ_u is less than 100 which allows at least two meters spacing between emitters. For any smaller values of α the maximum possible spacing is obviously larger. However in order to evaluate the actual spacing between the tricklers one has first to be able to estimate ρ_u (from equation [27] or [28]) before Wooding's solution can be applied.

Estimation of the radius of the ponded area ρ_u

An important boundary condition in [19] is the one concerning the size of the ponded water saturated area which is the only place where water can infiltrate into the soil. The boundary conditions [19d] through [19f] are mathematical expressions of the observation that, in general, a radial area of ponded water develops in the vicinity of the trickle source. This area is initially very small, but its radius $\rho(t)$ becomes larger as time increases (Figures 5 and 6). Since the ponded body of water is usually very thin, one can safely neglect the effect of storage of water at the soil surface. This means that the water from the trickle source is able to infiltrate into the soil, or evaporate into the air, instantaneously. Obviously, the soil water content immediately beneath the ponded area is always equal to the water content at saturation, θ_s.

From the numerical solution of equation [17] subject to the boundary conditions [19], vertical water fluxes at the soil surface ($z = 0$), across the saturated water entry zone $0 \leq r \leq \rho(t)$ has been obtained. It has been calculated (Brandt et al., 1971; Bresler, 1975) that this vertical water fluxes anywhere at $z = 0$ in the interval $0 \leq r \leq \rho(t)$ tend to approach a limit (see Figure 5 and 6). Since $\theta = \theta_s$ in this region, the hydraulic conductivity of the saturated zone is constant and equal to the saturated hydraulic conductivity K_s. Thus, the changes of water fluxes with time are due only to the changes in the hydraulic gradient at the surface. When these limits of water fluxes and hydraulic gradients are approached throughout the ponded area at $t \geq t_u$ then (neglecting E) we have from [19]

$$2\pi K_s(1 - \bar{G}) \int_0^{\rho_u} r dr = Q \qquad [26]$$

where $K_s = K(\theta_s)$ is the saturated hydraulic conductivity, $\rho_u = \rho(t \geq t_u)$ is the ultimate value of ρ at the time when surface fluxes approach their constant limits, Q is a constant trickle discharge, and $\bar{G}$ is the average surface pressure head gradients in the ponded zone defined by

$$\bar{G} = [\overline{dp/dz}]_{0 \leq r \leq \rho_u}^{z = 0} = \frac{1}{\rho_u} \int_0^{\rho_u} (dp/dz)_{z = 0} \, dr$$

Integrating [26] and rearranging, an equation for estimating the radius of the ponded-saturated water entry zone is obtained as

$$\rho_u = \{Q/[K_s(1 - G)\pi]\}^{1/2} \qquad [27]$$

Note that during infiltration the pressure head gradients are always less than or equal to zero. Hence

$$\rho_u = \sigma[Q/(\pi K_s)]^{1/2} \qquad [28]$$

where $\sigma = 1/(1 + |\bar{G}|)^{1/2}$. Obviously $0 < \sigma < 1$, however, in practice, a range of $0.5 < \sigma < 0.7$ has been generally obtained. Note that ρ_u is proportional to the square root of discharge, Q, and inversely proportional to the square root of saturated conductivity K_s. Equations [27] and [28], which give the relationships between ρ_u, Q, and K_s, are some of the important conclusions of the numerical solution of [17] and [19], (Brandt et al., 1971; Bresler, 1975).

Estimation of spacing between emitters

In order to estimate the actual spacing between emitters for a given set of field conditions the values of α, K_s and the desired value of $p = P_c$ midway between emitters must be known or estimated for any particular case.

Using these values one can calculate the distribution of S i.e, $S(\xi,\zeta)$, from which the desired spacing can then be detected. For convenience and designing purposes, it is generally sufficient to have the distribution of S at the soil surface, as given by $S(\xi,0)$ in Figure 11.

Figure 11 was reconstructed from Wooding's (1968) solution and gives the calculated distribution of S in terms of $S(\xi,0)/S_s$ as a function of α and ρ_u given by seven values of $a = \alpha\rho_u/2$. Because a unique relationship between S and θ and between θ and p (nonhysteritic case) exists, the data in Figure 11 represent also the soil surface distribution of water content as well as water pressure head. In order to obtain $p(r,0)$ and $\theta(r,0)$ values from Figure 11, when α, K_s and ρ_u are known, one has to use Figure 11, eq. [21] and the relationships

$$K = K_o + \alpha S_s(S/S_s) \qquad [29]$$

$$S_s = (K_s - K_o)/\alpha \qquad [30]$$

The values of θ can then be taken from the $\theta(p)$ relationship.

It should be noted that due to the linear form of [22], solutions from a single source as given in Figure 11 can be added together to solve for a more realistic situation of multiple sources field. Furthermore, the general solution to the linearized steady state form [22] of the flow equation [17] can be used for many particular and practical field problems The limitation of the linearized steady flow solution, on the other hand, is that the solution includes some errors due to the linearization procedure and to the steady flow assumption. The assumptions of no surface water flux away from the water entry zone and of constant σ value may also be inadequate for some field problems. In addition, it cannot be claimed that eq. [21]

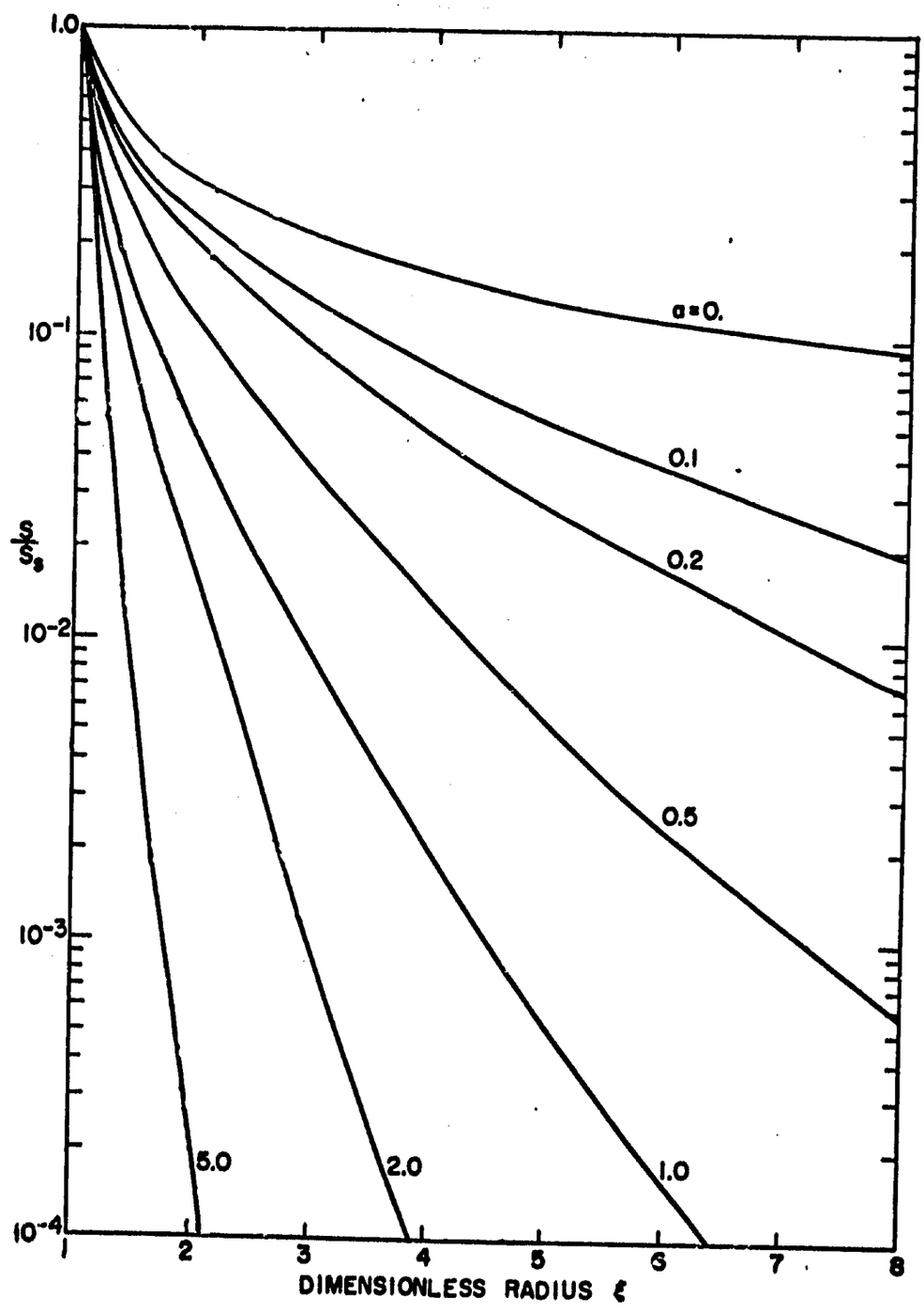

Figure 11. Soil surface values of S/S_s as a function of $\xi = r/\rho_u$ for different values of $\alpha = \alpha\rho/2$ (the numbers labeling the lines).

is universally exact, but according to Philip (1968) it does model the observed rapid nonlinear decrease of K with p in unsaturated soil. Values of α are generally smaller in fine textured material and larger in coarse-textured material where gravity may be relatively more important than capillary for water movement. However in spite of above mentioned limitations the steady state solution together with [27] may be useful in determining the spacing between emitters in the irrigated field according to the rate of discharge, the hydraulic properties of the soil, and the desired soil water pressure between emitters.

Numerical evaluation

Evaluation of the applicability of the proposed method must be obtained by comparing its results with real trickle infiltration field data. Since there have been no complete set of laboratory or field results reported in the literature, the results were compared with simulated data obtained by the numerical method proposed by Brandt et al. (1971). This is of course a first approach which should be fully examined in the field. Considering, however, the good agreement between the theory and experimental field and laboratory results, (Bresler et al., 1971) this approximation may be applicable to many field situations.

The parametric soil data given in Table 2 were taken from Bresler et al. (1971) for the two soils studied. In calculating $K(p_c)$ it was assumed that the relationship [21] holds for values of p which are smaller than the air entry value of each soil. Values of S were calculated from [29] when K values are substituted from [21], and S_s values from [30].

Table 2. Parametric soil data.

Soil	Air entry value of $p(p_a)$ (cm)	K_s (cm. min^{-1})	S_s (min^{-1})	α ($cm.^{-1}$)	Selected midway value		Value of p to be used in [21] $p_c = p(\theta_c) - p_a$	$K(p_c)$ (cm. min^{-1})	$S(p_c)/S_s$
					θ_c	$p(\theta_c)$ (cm)			
Gilat (loam)	-40	0.014	0.56	0.025	0.28	-80	-40	5.15×10^{-3}	0.367
Nahal-Sinai (sand)	-15	0.142	3.15	0.045	0.11	-55	-40	2.35×10^{-2}	0.166

Table 3. Estimated and calculated midway distances between the source for two soils and two rates of discharge.

Soil	Discharge, Q (liter/hr^{-1})	ρ_{est} 1/	ρ_{num} 2/	a 3/	$\xi(p_c)$ 4/ (dimensionless)	$[r(p_c)]_{est}$ 5/ (cm)	$[r(p_c)]_{num}$ 6/ (cm)
Gilat (loam)	4	22.6	27.6	0.28	1.41	39.0	33.1
	20	50.5	51.1	0.63	1.23	62.0	53.3
Nahal-Sinai (sand)	4	7.1	6.4	0.16	2.4	17.0	20.7
	20	16.1	17.5	0.36	1.95	31.4	29.3

1/Equation [27] with $\bar{G} = -2$ or [28] with $\sigma = 0.58$

2/The asymptotic $\rho(t_u)$ values of the numerical solution

3/$\alpha\rho_{est}/2$

4/From Figure 1 using $S(p_c)/S_s$ from Table 1 and pertinent "a"

5/$\xi(p_c)\rho_{est}$

6/Numerical calculation of radial distance at the soil surface to pertinent values of p_c given in Table 2

The soil parameters given in Table 2 were used to calculate the midway distance r_m corresponding to p_c for the two soils and two different trickle discharges using the data of Figure 11. The results of the estimated distances $r(p_c)$ are compared in Table 3 with numerical solution data of Bresler (1975) using values of $\sigma = 0.58$ or $|\bar{G}| = 2$ to calculate S_{est} data.

The data presented in Table 3 suggest that with the described estimation method one is able to approximate radial distances at the soil surface which corresponds to a given soil water pressure (or water content). It should be emphasized again that the proposed method is a good approximation to real field conditions as long as the numerical solution simulates the real field situations as has been previously shown in some specific cases (Bresler et al., 1971).

In summary, the present chapter suggests that steady and non-steady infiltration models, which are well suited for the analysis of unsaturated flow through porous media, can be applied to design trickle irrigation system. The combination of the two modeling approaches makes it possible to calculate the spacing between emitters as a function of their rate of discharge, soil hydraulic properties, and crop sensitivity to water stress. However, it is important to remember that the proposed method has certain limitations. For example, it involves errors that arise from the linearization procedure and from the estimation of ρ_u. Even more restricting is the assumption concerning the steady state flow. It is also emphasized that problems are involved in selecting the correct ρ_u. Additional research is needed to ascertain the validity of the views expressed in this study, to develop field methods for determining the necessary soil-water parameters, and to select the best mid-space pressure head for a given set of soil, climate, and crop growing conditions.

APPLICATION TO WATER MANAGEMENT IN TROPICAL SOILS

In many areas of the humid tropics soils are leached and become very acidic. Soil acidity is generally associated with aluminum toxicity which limits the rooting depth especially of those crops which are sensitive to aluminum. This limited rooting system is often accompanied by low values of "water holding capacity" and "available water content" (Charreau, 1974; Wolf and Drosdoff, 1974; Wolf, 1975). In these areas of humid tropics rains are generally adequate in total amount but frequently irregular in distribution. This unfavorable climatic-soil combination tends to produce soil-water deficits which in turn causes some degree of yield reduction (Wolf, 1975). In summarizing his experiments in soil-water properties at the Brasilia Experiment Station, Wolf (1975) concluded that water management is a critical factor for successful crop production in this region. This is so because of the unfavorable soil-water properties of these tropical soils in a combination with the occurrence of dry periods in the wet season and the limited root growth due to acidity and aluminum toxicity. Obviously crop yield cannot be obtained without irrigation during the dry season.

It appears therefore that since irrigation must be applied in these tropical areas trickle irrigation system may be preferred because of the following. The method is capable of delivering water into the soil in small quantities as often as desired so as to maximize frequency with no additional costs. As irrigation frequency increases, the infiltration period becomes the most important part of the irrigation cycle. When irrigation frequency is sufficiently high, so that irrigation cycle is dominated by

infiltration rather than by the extraction stage, the water holding capacity, or water availability properties of the soil become relatively unimportant. This is so because the soil water regime is continuously maintained in a relatively high water content level so that water is supplied to the crop as it is needed and there is no need to store water within the soil root zone (Rawlins, 1973). Not having to bring water from storage to the root zone also eliminates the negative effect of fluctuations in soil water content. Water management under high frequency trickle irrigation makes the unfavorable water storage properties of many tropical soils essentially unimportant. Irrigation management involves, therefore, optimization in the design of spacing between emitters and lateral system as well as control of the quantities of water to be applied in order to meet the crop requirements and the amount of water needed to pass through the root zone to avoid salinity buildup.

An additional problem typical to many tropical soils is that they have high capacity to fix phosphorus so as to make it unavailable to crops (Wolf, 1975). The low fertility status, high aluminum concentration, and phosphorus fixation create an additional serious soil limitation to agricultural development. This soil fertility problem may be controlled by applying fertilizers simultaneously with irrigation through the trickling system. By using the proper management practice, one is able to optimize this system with respect to the nutritional balance and water status.

The soil-water-crop information gained from experiments performed on Oxisols and Ultisols of Puerto Rico by Wolf and Drosdoff (1974) and on Dark Red Latosol in Brazil (Wolf, 1975) is used in this chapter for purposes of application of trickle irrigation principles to the design of trickle

irrigation system in these tropical soils.

Estimations of soil-water parameters

In order to design the trickling system in the field one must have first the parametric soil data K_s and α for any given field soil. The properties of three tropical soils to be used here are taken from the excellent work of Wolf and Drosdoff (1974) and Wolf (1975). The three soils are: (1) Carreras, clayey Ultisol from Puerto Rico; (2) Piña, sandy Oxisol from Puerto Rico and (3) Latosol Vermelho Escuro (LVE) or Dark Red Latosol (clay) from Brazil.

Data of capillary conductivity as a function of pore-water pressure head (in the range 10 to 80 cm H_2O) are presented in Figure 12. Measured data for Piña sand were taken from Table 3 (Appendix 2) of Wolf and Drosdoff (1974) for soil depth of 7.5 to 90 cm. Data points for Carreras clay are from Table 8 (Appendix 2) also for depths of 7.5 to 90 cm. Linear regression lines in the form $\ell nK = b + \alpha p$ were fitted to the data points of Piña with correlation coefficient of $r^2 = 0.96$. Very poor correlation ($r^2 < 0.15$) was found for Carreras soil. The straight line drawn in Figure 12 for this soil is not a regression line but a best visual fit to the data points. Substitute the values of b and α from the regression equation or from the best visual fit line then

$$K = 180.4 \exp(0.091p) \qquad \text{for Piña sand and}$$

$$K = 6.823 \exp(0.15p) \qquad \text{for Carreras clay soil.}$$

The line for the LVE soil drawn in Figure 12 were constructed from Figures 10 and 11 of Wolf (1975) for depth 0-45 cm in site II. From this line it appears that $K = 0.821 \exp(0.022p)$ for LVE soil. Note that the values of K for the three soils are in cm day^{-1}.

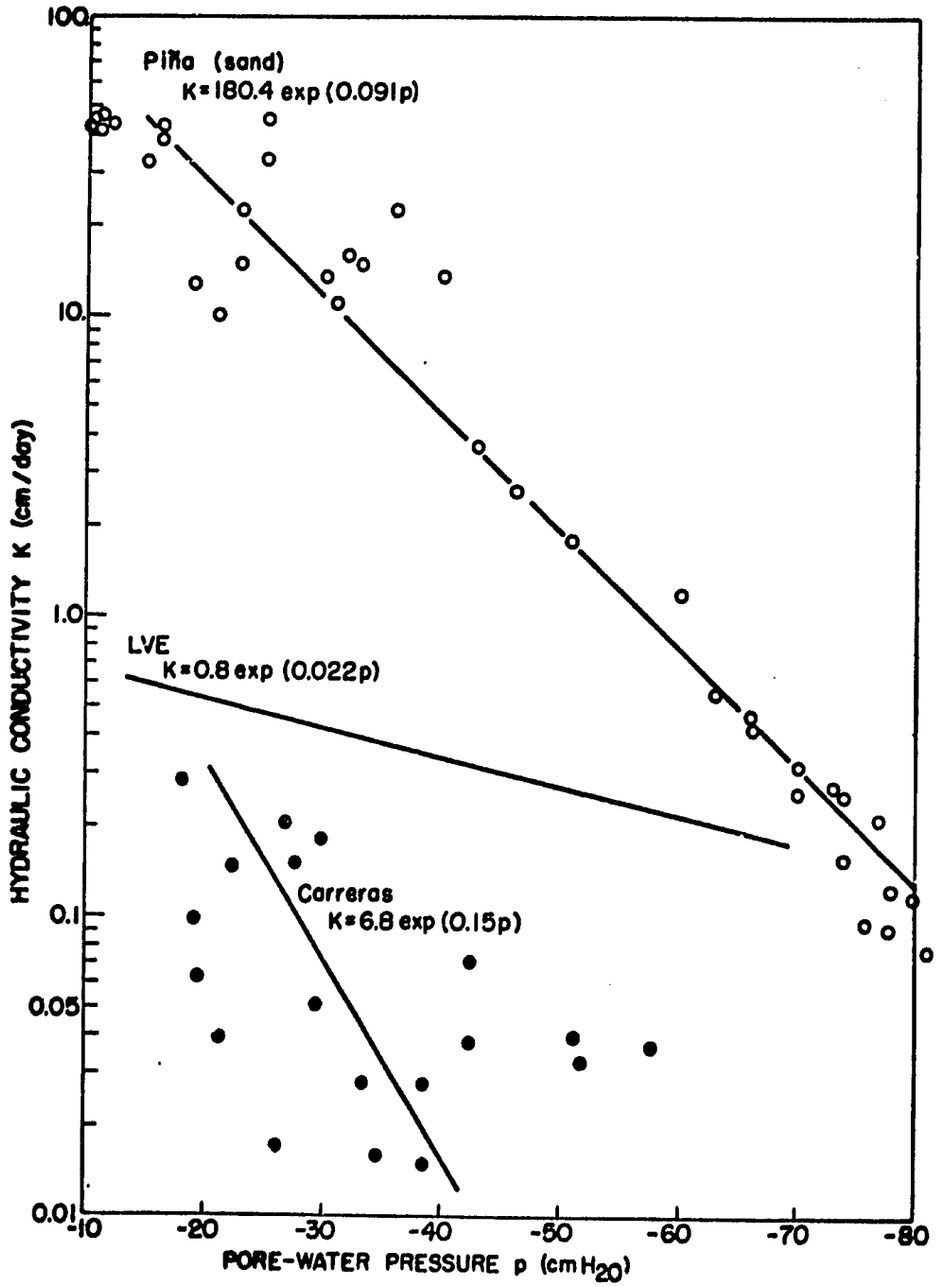

Figure 12. Unsaturated hydraulic conductivity as a function of pore-water pressure head. Data taken from Wolf and Drosdoff (1974) for Piña and Carreras soils and from Wolf (1975) for LVE soil.

Spacing between emitters as a function of discharge and midway pressure

Values of α and K_s estimated in the previous section were used to calculate the spacing between emitters as a function of the rate of trickle discharge and the desire water pressure p_c midway between emitters. To this goal the ultimate radius ρ_u of the ponded area must first be calculated. Figure 13 presents ρ_u as a function of the discharge Q for the three aforementioned tropical soils. From eq. [28] it is clear that for a given soil with a known K_s and σ, ρ_u is proportional to the square root of Q (and inversely proportional to $\sqrt{K_s}$ for a given value of Q). Thus the straight lines which diverge from the origin in Figure 13 are the functional relationship between ρ_u and $\sqrt{Q}$ the slope being equal to $\sigma\sqrt{24{,}000/\pi K_s}$ where K_s and Q are given in $cm \cdot day^{-1}$ and $liters \cdot hr^{-1}$, respectively. The effect of the saturated hydraulic conductivity of the soil on the ρ_u - Q relationship is clearly seen in Figure 13.

Values of α and K_s estimated for the Piña soil in Figure 12 were used to calculate the spacing between emitters as a function of trickle discharge and selected values of pressure head midway between emitters (Figure 14). Figure 14 may be used as a practical nomogram to calculate the distance between emitters if their rate of discharge is known, to select the desired discharge when spacing is given, or to find the best spacing-discharge combination when a certain economic criteria has to be achieved.

The general procedure of calculating the lines given in Figure 14 involves the following series of stages:

(1) Estimate K_s and α for any given soil (Figure 12).

(2) Estimate ρ_u as a function of Q (eq. [28], [29]) for any soil (Figure 13) using $\bar{G} = -2$ (or $\sigma = 0.58$) and the predetermined value of K_s.

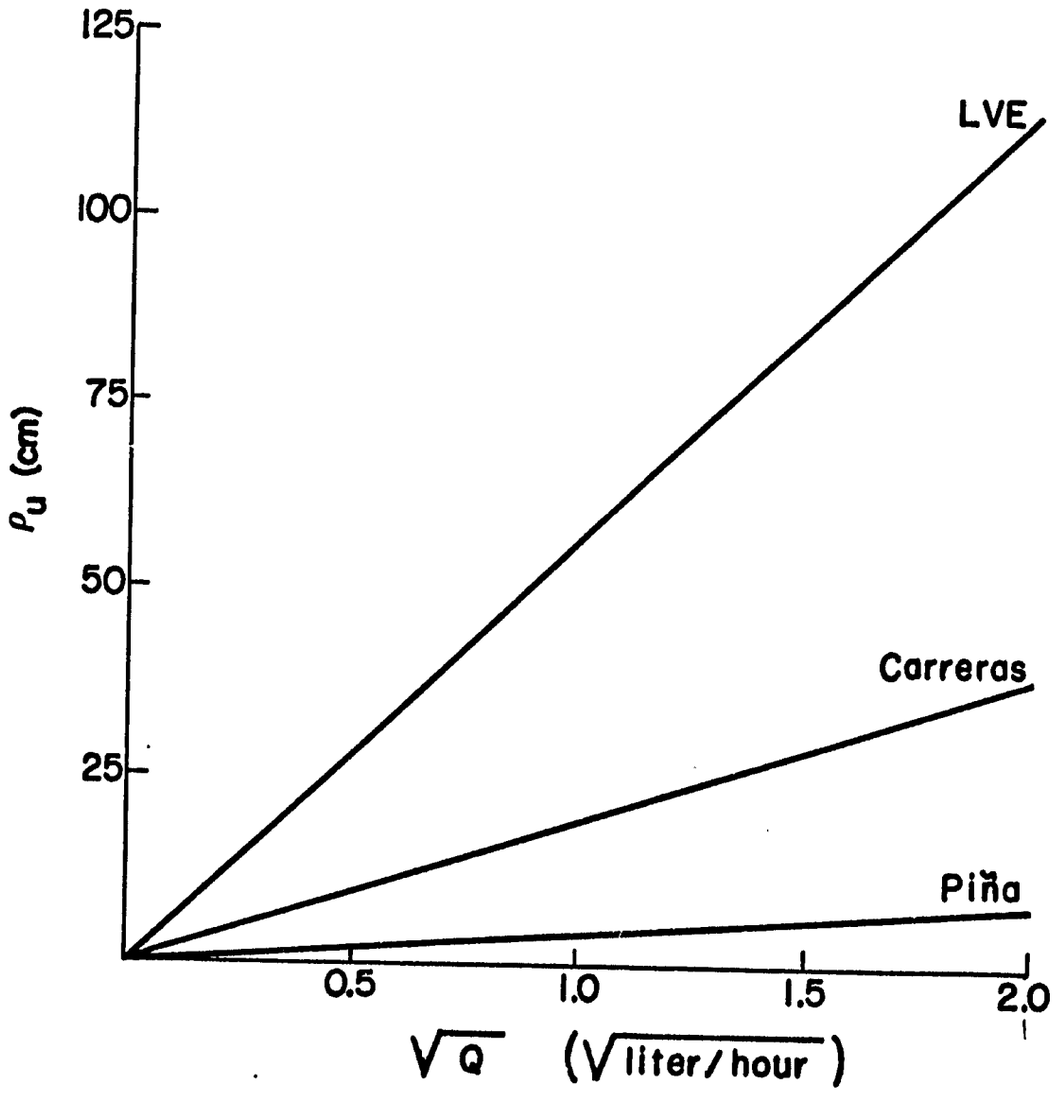

Figure 13. Ultimate radius of the ponded area ρ_u, as a function of the square root of trickle discharge for three tropical soils.

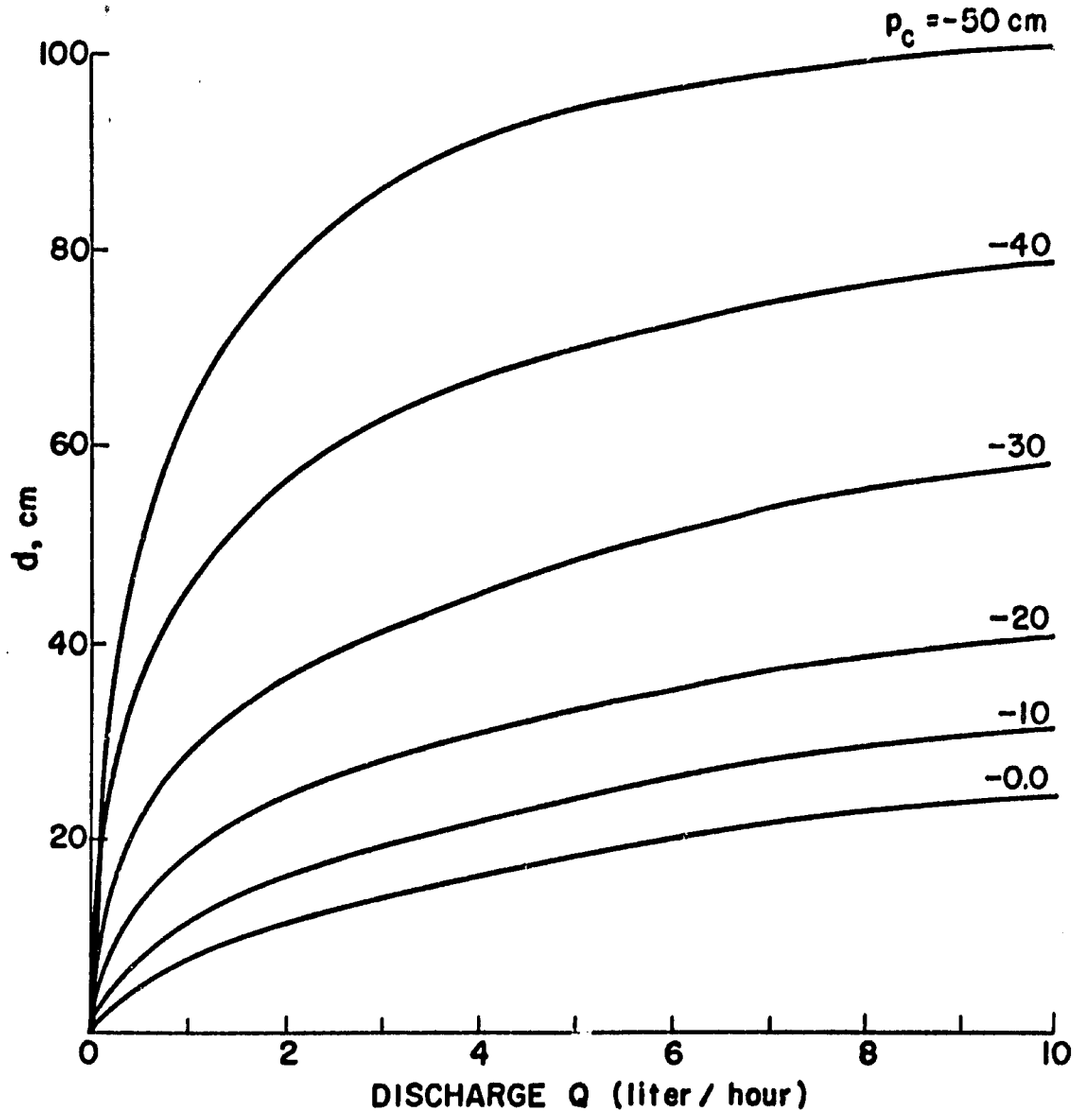

Figure 14. Estimated spacing between emitters $d = 2r(p_c,Q)$ as a function of trickle discharge, Q, and selected values of pore-water pressure head ($p = p_c$) midway between emitters (the numbers labeling the lines).

(3) Calculate $a = \rho_u(Q,K_s)\alpha/2$.

(4) Select a value of θ_c to be used and estimate p_c from the $p(\theta_c)$ characteristic curve, or select directly a value of p_c to be used.

(5) Calculate $K(p_c)$ from [21], S_s from [30] and $S(p_c)/S_s$ from [29] for every soil.

(6) Obtain $\xi(p_c)$ from Figure 11 using $S(p_c)/S_s$ and $a = \alpha p_u/2$. Note that $S(p_c)/S_s = [K(p_c) - K_o]/(K_s - K_o) \approx K(p_c)/K_s = \exp(\alpha p_c)$.

(7) Calculate the distance (spacing) between emitters as a function of the selected pressure head and trickle discharge, $d = 2r_m(p_c,Q)$, from $r_m = \xi_c \rho_u$.

(8) Plot the results (Figure 14).

In applying the results given in Figure 14 only one iso-p_c line must be used since any d - Q combination depends on the chosen value of p_c. This value must therefore be determined before any d - Q selection is made. The selection of p_c is somewhat arbitrary and depends on the safety factor that one would like to choose. This is so because of the uncertainty involved in the response of plants to p_c and to the degree of partial wetting of their root zone. It should be also remembered that in calculating the data of Figure 14 a single emitter (no interaction) was assumed. With this assumption a safety factor has already been taken no matter what value of p_c is chosen. As a general guideline it is recommended that the value of p_c to be selected is the one corresponding to the transition between the lowest and highest values of $\partial p/\partial r$ (i.e. when $|\text{grad } \theta|$ starts to increase steeply with r). In the case given in Figure 14 this lies between the iso-p_c lines of -20 and -30 or more precisely in the iso-p_c line of -25 cm. This is of course an average value which may be lower (more negative) for less sensitive crops

and must be higher when crops sensitive to water-stress are grown.

The effects of soil hydraulic properties on the spacing-discharge relationships are demonstrated in Figures 13 and 15. Figure 13 which represents the saturated-ponded water entry zone as a function of discharge for the three soils demonstrates the effect of K_s on the spacing-discharge relationships. The effect of α on the d-Q relationships when $p_c = -30$ cm H_2O is illustrated in Figure 15. According to Philip (1968) α is a measure of the relative importance of gravity and capillary for water movement in a particular soil. In soil with a high α value gravity tends to dominate and in soil with small α values capillary tends to dominate. That is the reason why at small discharges Q, values of d for LVE soils with a smaller α value tend to be less than d values for Carreras soil which has the highest value of α. Figure 15 also demonstrates the effects of soil water properties and rate of discharge on the selection of spacing between emitters. Larger spacing may be permitted in soils with higher values of K_s and α and also when the crop grown is not sensitive to partial soil wetting (higher p_c values are permitted). Smaller spacing is required in soils having smaller K_s and α when sensitive crop is being grown. At any given soil the emitter spacing can be increased as the discharge rate becomes higher. However since the rate at which r increases with Q is diminishing (Figures 14 and 15) the proper choice of Q depends mainly on some optimization criteria in the engineering design of the field irrigation system.

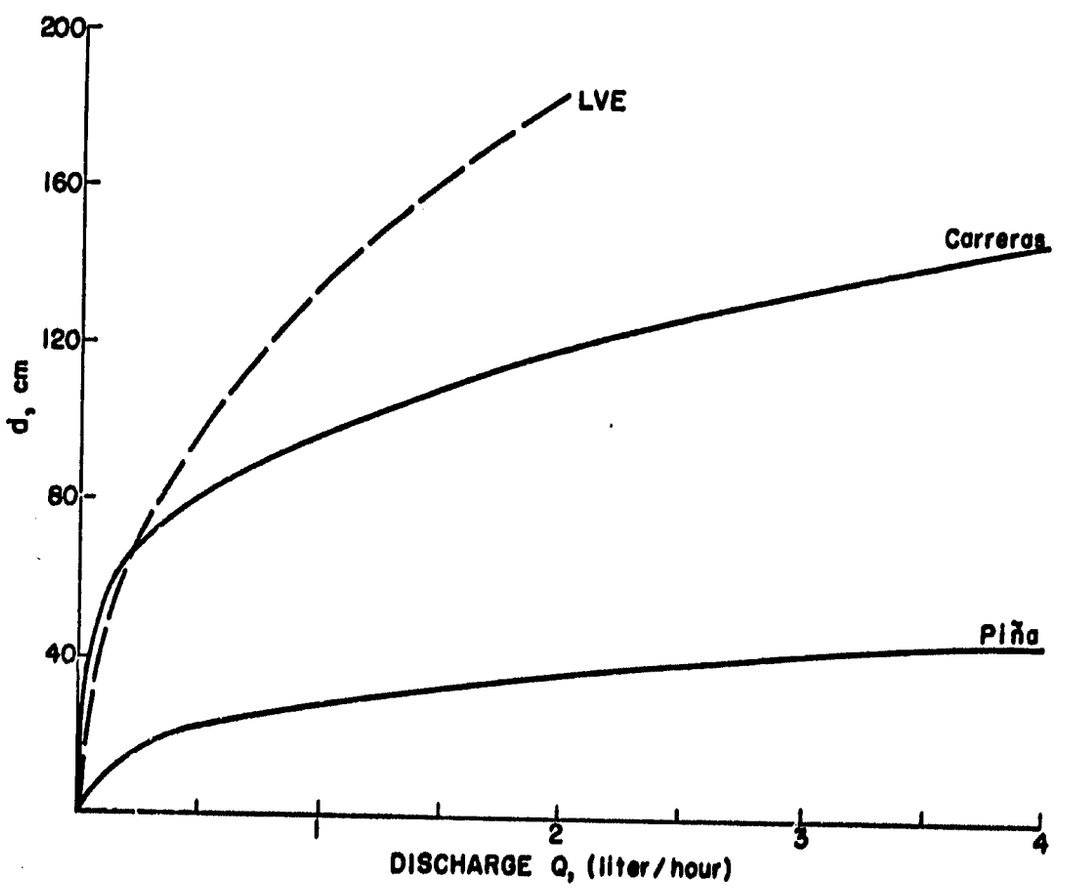

Figure 15. Distance between emitters as a function of trickle discharge for three tropical soils. (Value of p_c was taken to be -30 cm H_2O).

Irrigation scheduling

In this section Wolf's (1975) results for corn grown on LVE soil in Brazil will be considered as criteria for establishing irrigation schedules and practice for corn in similar tropical soils. The following discussion of irrigation frequency and quantity applies principally to a trickle-irrigated field when water is available on demand. The ratio between crop evapotranspiration (ET) and class A pan-evaporation, and the yield response to irrigation interval were taken from Wolf (1975) (Figures 25 and 21, respectively).

Figure 16 is actually a redrawing of Figure 22 of Wolf (1975) in which a visual fit line is added between the experimental data points, and extrapolated to a half-day interval. The dashed line in Figure 16 supports the views expressed by eq. [6] regarding irrigation frequency, trickle irrigation and crop yield response. It seems therefore (Figure 16) that an irrigation interval of one day or less may be the best choice for irrigation scheduling purposes.

The quantity of water to be applied by an emitter in each single irrigation for any day after planting is given by

$$q'(t) = R'(t)\ E_o(t)\ II(t)\ \pi r_w^2 \qquad [31]$$

when q' is the quantity of water to be applied by an emitter at the day t after planting, E_o is the class A pan evaporation between previous and present irrigation, II is the irrigation interval, r_w is the radius of area wetted by an emitter and $R(t) = ET(t)/E_o(t)$ is the ratio between evapotranspiration and E_o at the day t. This ratio as a function of number of days after planting is given in Figure 17 which is a reproduction of Figure 25 of

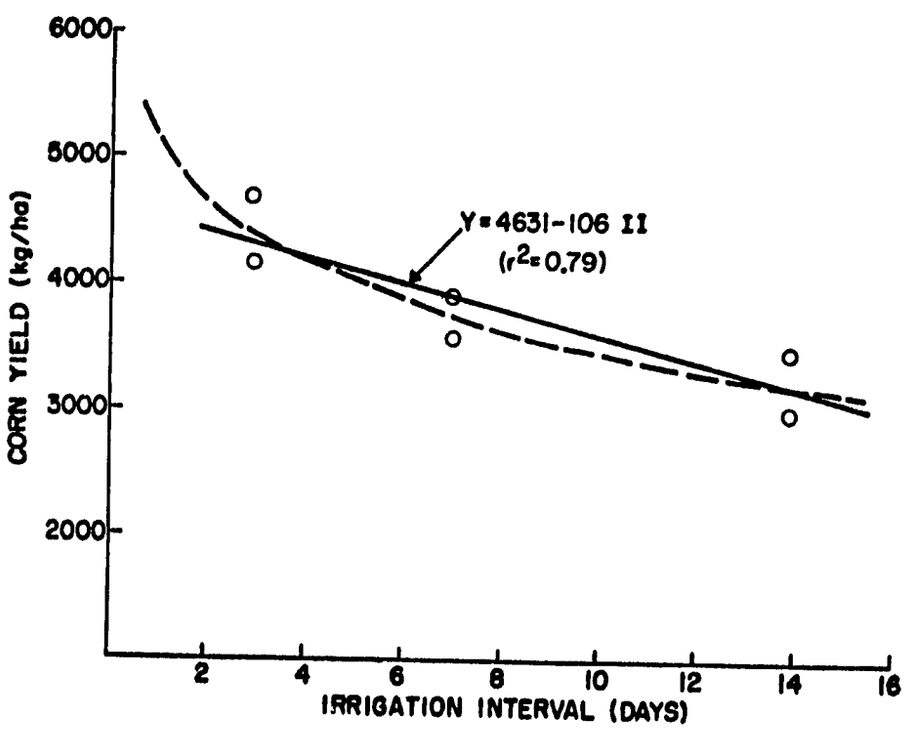

Figure 16. Yield of shelled corn as a function of irrigation interval (II) in dry season of Brasilia. Data points and regression solid line were taken from Wolf (1975). The dashed line is a visual fit-extrapolated line.

Wolf (1975). Note that if r_w (eq. [31]) is less than r_m (Figure 15) a certain water quantity must be added to q' in [31]. This is the quantity that must pass the root zone to avoid salinity buildup.

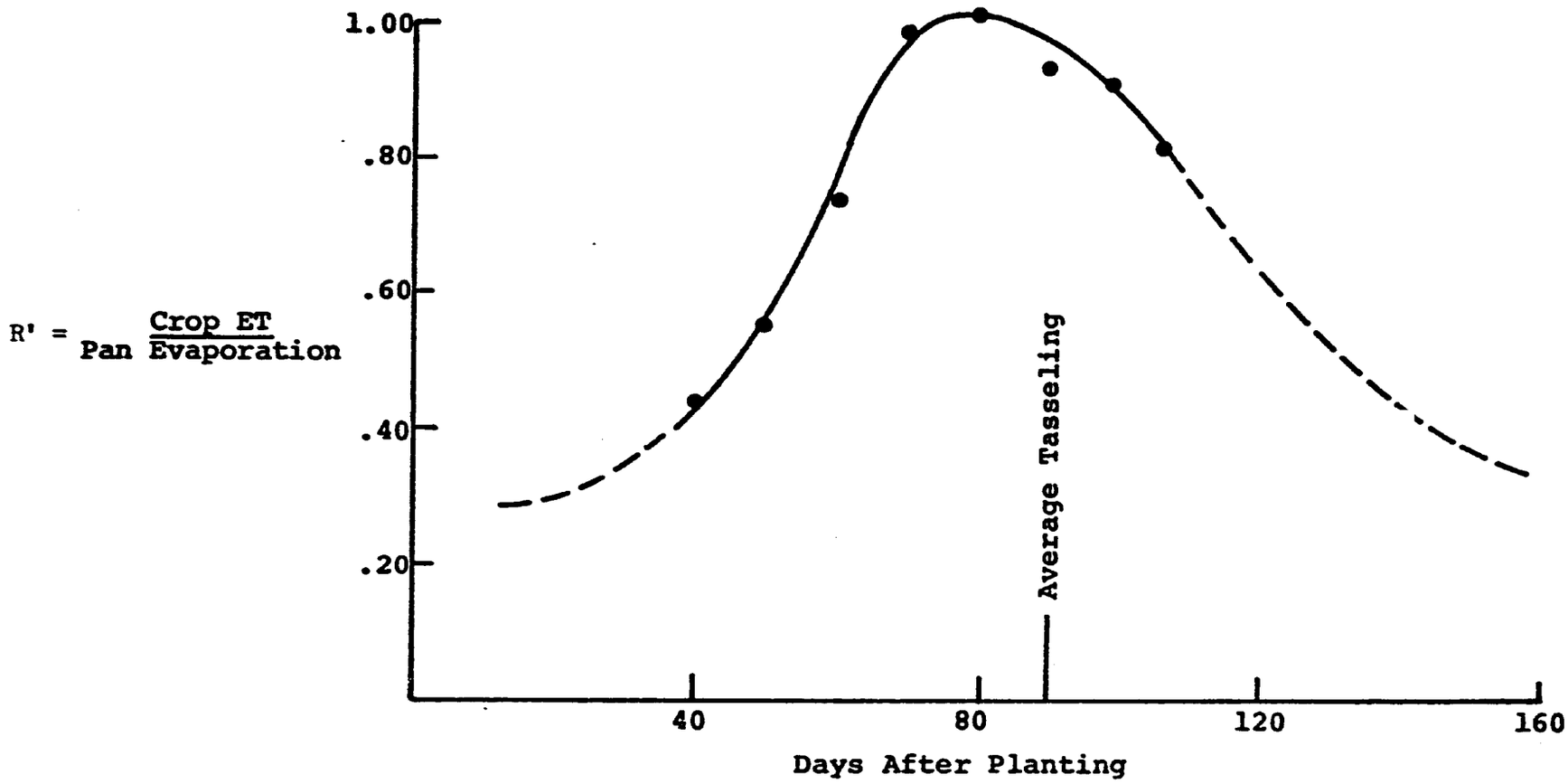

Figure 17. Ratio of crop ET to class A pan evaporation, R'(t) as a function of number of days after planting for well-watered dry season treatments (after Wolf, 1975).

Designing the lateral system

The data given in Figure 14 or 15 can be combined with principles of hydraulics in order to obtain diameter (D) and length (L) of the lateral system for designing purposes. For a given r_m - Q combination and uniformity criteria the L-D design relationship and the necessary pressure head at the lateral inlet depend upon emitter discharge function, elevation changes, reduction coefficient for dividing flow, and pipe roughness coefficient. Hayzen-Williams equation accounting for dividing flow between emitters is

$$H_L = 2.3173 \cdot 10^{-3} \cdot F \cdot L \cdot D^{-4.871} \, (\bar{Q}N/C)^{1.852} \qquad [32]$$

where H_L = friction pressure loss in laterals (PSi),

$\bar{Q}$ = average emitter rate of discharge (gallon hr^{-1}),

N = number of emitters per lateral,

F = reduction coefficient for dividing flow between emitters along the lateral,

L = the lateral length (ft),

D = inside diameter of the lateral pipe (inches),

C = the Hyzen-Williams roughness coefficient.

Equation [32] is an empirical equation so that there is no consistency in the dimensional system used. The dimensions assigned to each of the dimensioned variable above must be retained. The empirical values of F and C can be found in tables (see, for example, Howell and Hiller, 1974). The spacing between emitters along the lateral is given by $2r_m$ (Figure 15). It is possible therefore to express N as

$$N = \frac{L}{2r_m} = \frac{L}{d} \qquad [33]$$

where d is the distance between emitters along the lateral. Substituting L/d for N in [33] and rearranging

$$L = 8.394\ D^{1.708}\ (H_L/F)^{0.3506}\ (Cd/\bar{Q})^{0.6494} \qquad [34]$$

Knowing the $\bar{Q}$ - d relationship from Figure 15 and assuming F to be constant over any given range of L and d, equation [34] gives the L - D relationships for any preselected value of head loss H_L.

A proper criteria in order to select the appropriate value of H_L for [34] may be based on the differences between the emitter discharge at the lateral inlet and the downstream discharge, relative to the average discharge. these criteria are taken then

$$\frac{Q_i - Q_d}{\bar{Q}} \leq \varepsilon \qquad [35]$$

where Q_i is the inlet discharge, Q_d is the downstream discharge, and ε is a preselected fraction, say 0.05 or similar.

The orifice discharge equation is

$$Q = C_q A\sqrt{2gH}$$

where Q here is the discharge at the orifice, A its area, C_q its discharge coefficient, H total hydraulic head, and g acceleration due to gravity. Due to the geometry of the flow path through the emitter, the relationship between emitter discharge rate and the hydraulic head at the emitter may be given by the empirical expression

$$Q = bH^{\beta} \qquad [36]$$

where b and β are constant characteristics of the flow regime in the emitter

and H is the hydraulic head at the emitter. Data of a and β are available from the manufacturer but also can easily be determined empirically in the laboratory.

Using the maximum value of ε it follows from [35] using [36] that

$$H_i^{\beta} = \frac{\varepsilon Q}{b} + H_d^{\beta} \qquad [37]$$

Since $H_L = H_i - H_d$ then

$$H_i^{\beta} = \frac{\varepsilon \bar{Q}}{b} + (H_i - H_L)^{\beta} \qquad [38]$$

Thus, by knowing the pressure head at the lateral inlet and the emitter constants b and β the value of H_L can be calculated from [38] for given ε and $\bar{Q}$ (Figure 15). This value of H_L is then substituted into [34] to calculate the D - L relationship needed for the lateral design. Thus when the lateral length is given by the size of the plot and H_i is known, the diameter D is calculated from [34]. Otherwise the optimum economic D-L-H_i combination has to be calculated for any field and soil conditions.

LITERATURE CITED

Ayers, A. D., C. H. Wadleigh and C. C. Magistad. 1943. The interrelationships of salt concentration and soil moisture content with the growth of beans. J. Amer. Soc. Agron. 35:796-810.

Bear, J. 1972. Dynamics of fluids in porous media. pp. 579-662. American Elsevier, New York.

Black J. D. F. and D. W. West. 1974. Water uptake by an apple tree with various proportions of the root system supplied with water. Proc. 2nd Int. Drip Irrig. Congress 74:432-436.

Bernstein, L. and L. E. Francoios. 1973. Comparisons of drip, furrow and sprinkler irrigation. Soil Sci. 115:73-86.

Brandt, A., E. Bresler, N. Diner, I. Ben-Asher, J. Heller, and D. Goldberg. 1971. Infiltration from a trickle source. I. Mathematical models. Soil Sci. Soc. Amer. Proc. 35:675-682.

Bresler, E. 1973. Simultaneous transport of solute and water under transient unsaturated flow conditions. Water Resour. Res. 9:975-986.

Bresler, E. 1975. Two-dimensional transport of solutes during nonsteady infiltration from a trickle source. Soil Sci. Soc. Amer. Proc. 39: (in press).

Bresler, E., J. Heller, N. Diner, I. Ben-Asher, A. Brandt, and D. Goldberg. 1971. Infiltration from a trickle source: II. Experimental data and theoretical predictions. Soil Sci. Soc. Amer. Proc. 35:683-689.

Bresler, E. and D. Russo. 1975. Two-dimensional solute transfer during nonsteady infiltration: Laboratory test of mathematical model. Soil Sci. Soc. Amer. Proc. 39: (in press).

Bresler, E. and D. Yaron. 1972. Soil water regime in economic evaluation of salinity in irrigation. Water Resour. Res. 8:791-800.

Charreau, C. 1974. Soils of tropical dry and dry-wet climatic areas of West Africa and their use and management. Agronomy Mimeo 74-26. 434 pp. Dept. of Agronomy, Cornell University.

Gustafson, C. D., A. W. Marsh, R. L. Branson, and S. Davis. 1974. Drip irrigation--worldwide. Proc. 2nd Int. Drip Irrig. Congress 74:17-22.

Frith, G. J. T. and D. G. Nichols. 1974. Effects of N-fertilizer applications to part of a root system. Proc. 2nd Int. Drip Irrig. Congress 74:434-436.

Hanks, R. J., A. Klute and E. Bresler. 1969. A numeric method for estimating infiltration, redistribution, drainage, and evaporation of water from soil. Water Resour. Res. 5:1064-1069.

Hillel, D. 1972. The field water balance and water use efficiency. IN Optimizing the soil physical environment toward greater crop yields. (D. Hillel, ed.). Academic Press, N.Y. pp. 79-100.

Howell, T. A. and E. A. Hiler. 1974. Trickle irrigation lateral design. Transactions of the ASAE, 17:902-908.

Lange, A., F. Aljibury, and B. Fischer. 1974. Weed control under drip irrigation in orchard and vineyard crops. Proc. 2nd Int. Drip Irrig. Congress 74:422-424.

Neuman, S. P. 1973. Saturated-unsaturated seepage by finite elements. Proc. ASCE, J. Hydrol. Div. 99, HY12:2233-2250.

Ogata, A. 1970. Theory of dispersion in a granular medium. Geological Survey Professional Paper 411-I, 34 pp., U.S. Govt. Printing Office, Washington, D.C.

Perkins, T. K. and O. C. Johnston. 1963. A review of diffusion and dispersion in porous media. Soc. Petrol. Eng. J. 3:70-84.

Philip, J. R. 1968. Steady infiltration from buried point sources and spherical cavities. Water Resources Research, Vol. 4, No. 5, Oct., pp. 1039-1047.

Rawitz, E. 1970. The dependence of growth rate and transpiration rate on plant and soil physical parameters under controlled conditions. Soil Sci., Vol. 110, No. 3, Sept., pp. 172-182.

Rawlins, S. L. 1973. Principles of managing high frequency irrigation. Soil Sci. Soc. Amer. Proc., Vol. 37, No. 4, July-Aug., pp. 626-629.

Taylor, S. A. 1952. Use of mean soil moisture tension to evaluate the effect of soil moisture on crop yields. Soil Sci. 74:217-226.

Talsma, T. 1963. The control of saline ground water. Mededel. Landbouwhogeschool Opzoekingsta. Staat. Gent, Wageningen, 63(10), pp. 1-68.

Tranter, C. J. 1951. Integral transformations in mathematical physics. Methusuen Press, London, 133 pp.

Wadleigh, C. H. and A. D. Ayers. 1945. Growth and biochemical composition of bean plants as conditioned by soil moisture tension and salt concentration. Plant Physiol. 20:106-132.

Wadleigh, C. H., H. G. Gandi, and M. Kolisch. 1951. Mineral composition of orchard grass grown on Pachappe loam salinized with various salts. Soil Sci. 72:275-282.

Willoughby, P. and B. Cockroft. 1974. Changes in root patterns of peach trees under trickle irrigation. Proc. 2nd Int. Drip Irrig. Congress 74:439-445.

Wolf, J. M. and M. Drosdoff. 1974. Soil-water studies on Oxisols and Ultisols of Puerto Rico. Agronomy Mimeo 74-22, Depts. of Agronomy and Agr. Engineering, Cornell University, Ithaca, N.Y. 14853, August, 58 pp.

Wolf, J. M. 1975. Water constraints to corn production in central Brazil. Ph.D. Thesis, Cornell University.

Wooding, R. A. 1968. Steady infiltration from a shallow circular pond. Water Resour. Res., Vol. 4, No. 6, Dec., pp. 1259-1273.

Zentmyer, G. A., F. B. Guillemet, and E. L. V. Johnson. 1974. The relation between drip irrigation, Phytophthora root rot of avocado, and fungicides. Proc. 2nd Int. Drip Irrig. Congress 74:512-514.

Zaslavsky, D. 1972. Analysis of growth parameters and their fluctuations in searching for increased yields. In Optimizing the soil physical environment toward greater crop yields, (D. Hillel, ed.) Academic Press, N.Y., pp. 223-232.

APPENDIX - NOTATIONS USED

The following symbols are used in this paper:

$a = \alpha\rho_u/2$ = parameter proportional to the length scale, dimensionless;

b = constant, L^2T^{-1};

c = solute concentration in the soil solution, ML^{-3};

C = Hayzen-Williams roughness coefficient;

C_o = solute concentration of the irrigation water, ML^{-3};

D = inside diameter of the lateral pipe, L;

d = distance between emitters along the lateral, L;

D_p = soil diffusion coefficient, L^2T^{-1};

D_{ij} = hydrodynamic dispersion tensor, L^2T^{-1};

E = evaporation flux, LT^{-1};

E_o = class A pan evaporation rate, LT^{-1};

ET = evapotranspiration rate, LT^{-1};

F = reduction coefficient for dividing flow, dimensionless;

$\bar{G}$ = average pressure head gradient over the ponded area at the soil surface, dimensionless;

H = hydraulic head, L;

H_i = inlet pressure, $ML^{-1}T^{-2}$;

H_d = downstream pressure, $ML^{-1}T^{-2}$;

H_L = pressure loss in lateral, $ML^{-1}T^{-2}$;

II = irrigation interval, T;

K^s_{ij} = saturated hydraulic conductivity tensor, LT^{-1};

$K_r(\theta)$ = relative hydraulic conductivity, dimensionless;

$K = K(\theta) = K(p) = K_r(\theta)K^s$ = capillary conductivity in isotropic media, LT^{-1};

L = lateral length, L;

N = number of emitters per lateral, dimensionless;

p = pore-water pressure head, L;

Q = f(t) = rate of discharge from emitter, L^3T^{-1};

Q_i = inlet discharge, L^3T^{-1};

Q_d = downstream discharge, L^3T^{-1};

q = specific solution flux (Darcy's velocity), LT^{-1};

q' = quantity of water to be applied by an emitter, L^3;

r = radial coordinate, L;

R = radial boundary of flow region, L;

R' = ratio between evapotranspiration and class A pan evaporation, dimensionless;

r_w = radius of the wetted area, L;

r_m = half distance between emitters, L;

$S = S(\theta) = S(p)$ = transform water content, transform pore-water pressure head, L^2T^{-1};

t = time, T;

T = end time of infiltration, T;

x_i = Cartesian coordinate, L;

x_3 = vertical coordinate, L;

x,y = horizontal coordinates, L;

Y = crop yield per unit land area, ML^{-2};

V = average solution flow velocity, LT^{-1};

z = vertical coordinate, L;

Z = vertical boundary of flow region, L;

α = constant, L^{-1};

β = constant, dimensionless;

ζ = relative vertical coordinate, dimensionless;

θ = volumetric water content, dimensionless;

Φ = soil-water regime index, dimensionless;

$\bar{\Phi}$ = average value of Φ, dimensionless;

ϕ = deviation of Φ from $\bar{\Phi}$, dimensionless;

ε = discharge difference fraction, dimensionless;

σ = constant, dimensionless;

σ^2 = variance of $\phi(t)$, dimensionless;

λ_L = longitudinal dispersivity, L;

λ_T = transversal dispersivity, L;

ξ = relative radial coordinate, dimensionless; and

ρ = radius of the ponded-water entry zone, L.

<u>Subscripts</u>:

o = reference value usually air dry water content,

n = initial value,

s = value at saturation,

u = ultimate value, limiting value, and

c = selected midway value.